

Optimization of Kiln Feed Yield through an Analysis of Drilling and Blasting Parameters in a Quarry

By

A. Waheed

in partial fulfilment of the requirements for the degree of

Master of Science

In Resource Engineering

(European Mining Course)

at the Delft University of Technology,

Supervisor: Dr. M. Buxton TU Delft

Thesis committee: Dr. A. Hennig, RWTH Aachen University

Dr. R. S. Guerrero, Aalto University

Mr. L. Weimer, RWTH Aachen University

An electronic version of this thesis is available at <http://repository.tudelft.nl/>.

1 ACKNOWLEDGEMENT

The thesis would not have been possible without the support of a great many people who on course, to where I stand today, have provided me with guidance, advise and all the necessary input, I needed.

First of all, I thank Lhoist S.A. for entrusting me with the opportunity to work with them. The independence, exposure and support the company has provided me has helped me greatly throughout the period and has proven to be great learning opportunity for me as a student and as an individual.

I acknowledge the kind support and feel honoured with the welcoming and hospitable attitude of the team at Jemelle. Their cordial behavior helped me a lot in making myself comfortable and staying focused on the task at hand. Additionally, I would extend my gratitude towards Mr. Emmanuel Hoyez, whose cooperation has helped in materializing the study at Jemelle.

Nothing would have been possible without the undue support and advise of Mr. Jean Materne and Mr. Christophe Delneuville, their outright encouragement and facilitation has given me great confidence and made this project what it is. I specially would mention Ms. Otto Grasiela, who always took great interest in the project and provided me with the most constructive feedback and support in my study.

Shout out to my colleagues of EMC, to whom I owe greatly for the support, guidance and above all the fun I had, during the period.

I thank my family the most, for keeping their faith in me and letting me pursue my dreams.

Thank you

Atif Waheed

August 2019

Delft, Belgium

2 ABSTRACT

Blasting and drilling serves as an essential element for a mining operation to excel. Optimization of this operational aspect, requires consideration of various parameters that can be controllable or uncontrollable. To overcome the tediousness of analyzing each element selectively, some major parameters are outlined, and each blast is rendered relative to the other, by organizing the data from each blast design and integrating it in an empirical model called Kuz-Ram Model, which further can be used for predicting the impact of these parameters on fragmentation. Image analysis aids in validating the model credibility for using it as step forward for proposing alterations to the current practices in drilling and blasting area. Each image is processed with the help of Unmanned Aerial Vehicle, for safety and coverage of complete muck-pile.

The study involves in depth focus on the impact of rock mass characteristic over fragmentation as well. Discontinuities, fractures, joint orientation and fillings are considered in designating each rock zone to specific class with the help of a geo-mechanical classification system called, Rock Mass Rating. To test the theory, an exercise is performed by separating two zones of variable rock mass properties and then the procedure is followed with empirical calculation, image analysis and supported by preferential loading to acquire a broad image of each zone fragmentation profile. Suggesting the variation in particle size distribution due to rock mass influence. The collected data and analyses shall serve as supporting tools for changes to blast design for obtaining desired fragmentation, which is synonymous to increasing the feed of kilns.

TABLE OF CONTENTS

1	Acknowledgement	III
2	Abstract	IV
1	Introduction.....	1
1.1	Objective	2
1.2	2
1.3	Scope & Limitations	2
2	Literature Review.....	4
2.1	Drilling and Blasting	4
2.1.1	Uncontrollable Parameters	4
2.1.2	Geometric Parameters.....	6
2.1.3	Explosives	9
2.2	Fragmentation Model	12
2.3	Image Analysis.....	14
2.4	UAVS in Mining.....	17
3	Industrial Case.....	19
3.1	Jemelle site	19
3.1.1	Geology	19
3.1.2	Lime Processing Plant.....	25
3.1.3	Kilns.....	27
3.2	Case for Jemelle	30
4	Theoretical Approach.....	32
4.1	Purpose and Methodology	32
4.2	Results and discussion	33
4.2.1	Sensitivity Analysis	33
4.2.2	Burden.....	33
4.2.3	Spacing.....	34

4.2.4	Powder Factor	34
4.2.5	Drill-Hole diameter	34
4.2.6	Burden/Spacing Ratio	35
4.2.7	Specific Explosive Energy	36
4.2.8	Bench Height	36
5	Model Validation	39
5.1	Purpose and Methodology	39
5.2	Results and Discussion	42
5.2.1	Correlation and RMS	47
5.2.2	Belt Scale Data Test	48
6	Correlation between Rock Mass and Fragmentation	50
6.1	Purpose and Methodology	50
6.2	Results and discussion	54
6.2.1	Point Load Strength Test	54
6.2.2	Rock Mass Rating	55
6.2.3	Rock Factor	55
6.2.4	Fragmentation	56
6.2.5	Conclusion	59
7	Way Forward	60
8	Conclusion	66
9	Recommendations	68
10	References	70
11	Appendix	i
11.1	Blast Parameters	i
11.2	Wipfrag analysis	ii
11.3	Point Load Test	iv
11.4	Rock Mass Rating	vi

11.5	Rock Factor	vii
11.6	Explosives.....	x
11.7	Regression Analysis	xi
11.8	Fines Area Calculation.....	xiii
11.9	Rock Mass Tracing	xiv
11.10	Fragmentation.....	xvii

TABLE OF FIGURES

Figure 1; Geometry of Blasting (Ash 1963)	9
Figure 2 Effect of hole-to-hole delay on fragmentation (SME, 2011).....	11
Figure 3 Effect of simultaneously fired holes splitting at S/B ratio of less than 2:1; (fracture face coalesces and provide a split before fracturing reaches the free face) (SME, 2011)	12
Figure 4 Measurement of Ground Sample Distance (Dering, 2019)	18
Figure 5 Geological map of southern Belgium showing main Frasnian buildups, where La Boverie quarry is represented by number 6 encircled in red (Boulvain et al., 2005)	20
Figure 6 S-N cross-section and lithostratigraphic subdivisions of the Frasnian of the Dinant Synclinorium (Boulvain and Coen-Aubert, 2006)	21
Figure 7 Sedimentological model by Boulvain et al., 2005	23
Figure 8 A NW-SE cross-section map of the La Boverie quarry representing the carbonate mounds (Lhoist S.A.)	24
Figure 9 A cross-sectional view of the exposed mining faces from La Boverie quarry representing the three units, the measurement of scale is approximate.	24
Figure 10 Processing Plant Flow Diagram – Jemelle (Lhoist S.A.)	26
Figure 11 Washing Plant Flow Diagram (Lhoist S.A.)	27
Figure 12 Schematic diagram of a parallel flow regenerative Maerz kiln where (a) fuel; (b) combustion air; (c) cooling air; (d) kiln gases; (e) air duct; (f) shaft 1; (g) shaft 2 (Oates, 2008)	28
Figure 13 Annular shaft kiln where (a) upper burners; (b) lower burners; (c) combustion air to upper burners; (d) combustion air to lower burners (e) kiln exhaust gases (Oates, 2008)	30
Figure 14 Sensativity Analysis for Different Paramters	33
Figure 15 Burden-spacing Ratio impact on Fine generation.....	35
Figure 16 Impact of Bench Height over fragmented size.....	37
Figure 17 Bench height Impact on Particle Mean Size	38
Figure 18 Discontinuities Sketching (Red: Discontinuity; Yellow: Filling), for scale use grid size 5m x 5m	39
Figure 19 Face Zonal Division.....	41
Figure 20 Fragmentation Zonal Division.....	41
Figure 21 WipFrag Analysis for F2H Blast on April 4th, 2019	42

Figure 22 Wipfrag Analysis for Compressed Image of F2H Blast 4/4/19.....	43
Figure 23 Analysis sample area from Blast 1, Left, original; Right, detected particles; color scheme denotes the size, red being largest and blue the smallest.....	44
Figure 24 Wipfrag analysis following the reduced region exercise, result of 9 images merged together; F2H 5A, 4-4-19	44
Figure 25 Comparison between empirical method and image analysis F2H 5A, 4-4-19	45
Figure 26 Comparison between the empirical methods and Image Analysis F2H 5B, 15-5-19.....	46
Figure 27 Comparison between empirical method and image analysis F2H 5A, 16-5-19	46
Figure 28 Comparison between empirical method and image analysis F2D 4, 23-5-19	47
Figure 29 Zones from the bench; Right, Zone 1; Left, Zone 2.....	52
Figure 30 Zones from the bench, after blast was performed; Right, Zone 1; Left, Zone 2	53
Figure 31 Point Load Testing Results for Each of the Two Zones	54
Figure 32 PSD prediciton using Kuz-Ram Model	57
Figure 33 PSD for the Zones using Image Analysis	57
Figure 34 Zonal view of the fragmentation after preferential loading cycles were followed.....	58
Figure 35 Difference in fragmentation with changed S/B ratio for F2H 5e bench, Blast of same bench on 16/5/19.....	61
Figure 36 Difference in fragmentation with changed S/B ratio for F2D 4, Blast of same bench on 23/5/19	61
Figure 37 Image Analysis Result Comparison	62
Figure 38 Difference in charge length between theoretical and actual; Left, Theoretical; Right, Actual (Schematic)	64
Figure 39 Example Image showing cracks post blasting in the crest region	64
Figure 40 WipFrag Analysis for Blast 1, 9 images merged together; F2H 5A, 4/4/19 ..	ii
Figure 41 WipFrag Analysis for Blast 2, result from 11 merged images; F2H 5B, 15/5/19	ii
Figure 42 WipFrag Analysis for Blast 3, result from 7 merged images; F2H 5A, 16/5/19	ii

Figure 43 WipFrag Analysis for Blast 4, result from 22 merged images; F2D 4, 23/5/19	iii
Figure 44 WipFrag Analysis for Zonal Exercise, result from 4 merged images; Zone 1, F2D 4, 23/5/19	iii
Figure 45 WipFrag Analysis for Zonal Exercise, result from 4 merged images; Zone 2, F2D 4, 23/5/19	iii
Figure 46 Example of Samples for Point Load Test Prior test and post-testing	iv
Figure 47 Point load strength for Blast 1 bench	iv
Figure 48 Point Load Strength for Blast 2 bench.....	iv
Figure 49 Point Load test for Blast 3 bench	v
Figure 50 Point Load test for Blast 4 bench	v
Figure 51 Rock Mass Rating, Classification of Rock Masses (Bieniaswki, 1989)	vi
Figure 52 Rock Factor Calculation; Green cells indicate the input data for measurement	ix
Figure 53 Supporting Data for Rock Factor Calculation	ix
Figure 54 Regression Analysis for Blast 1, 4/4/19.....	xi
Figure 55 Regression Analysis for Blast 2, 15/5/19.....	xi
Figure 56 Regression Analysis for Blast 3, 16/5/19.....	xii
Figure 57 Regression Analysis for Blast 4, 23/5/19.....	xii
Figure 58 Image of Fragmentation, with white region distinguishing the fines area.	xiii
Figure 59 Schematic of inscribed circle method.....	xiii
Figure 60 Rock Mass Discontinuity Tracing using ImageJ; 4/4/19, For scale use Grid Size, 5m x 5m	xiv
Figure 61 Rock Mass Discontinuity Tracing using ImageJ; 15/5/19, for scale use Grid size 2m x 2m	xv
Figure 62 Rock Mass Discontinuity Tracing using ImageJ; 23/5/19; For scale use Grid Size 4m x 4m	xvi
Figure 63 Fragmentation from Blast 1	xvii
Figure 64 Fragmentation from Blast 2.....	xvii
Figure 65 Fragmentation From Blast 3.....	xviii
Figure 66 Fragmentation from Blast 4.....	xviii

TABLE OF TABLES

Table 1 Description of the six build facies and three flanking facies defined by Boulvain et al., 2005	21
Table 2 Kiln feed and Capacity details	28
Table 3 Blast Fragmentation Fraction, by back calculation from total production (Materne, 2018).....	31
Table 4 RMR Values for Each Zone in the Bench Face	40
Table 5 Fine particles representation in the fragmentation pile for each day of imaging for F2H 4/4/19 Blast	43
Table 6 Correlation and RMS values for Empirical and Image Analysis	47
Table 7 Belt Scale Data Test Results (Jemelle Plant, 2018)	48
Table 8 Comparison of Model Results with Belt Scale Data Tests.....	49
Table 9 Comparison of Zonal Data Collected.....	56
Table 10 Belt Scale data from Stone Preparation Plant	58
Table 11 Parameters comparison between F2D 4e and F2H 5e	62
Table 12 Blast Parameters for the four blasts analyzed	i
Table 13 Rock Factor Measurement Parameters (S.Gheibe, H.Aghababa, & S.H.Hoseini, 2009)	vii
Table 14 Explosives characteristics	x
Table 15 Average RMR values for each zone in Bench Blasted 4/4/19	xiv
Table 16 Average RMR values for each zone in Bench Blasted 15/5/19	xv
Table 17 Average RMR values for each zone in Bench Blasted 23/5/19	xvi

1 INTRODUCTION

Drilling and blasting holds major importance in any mining operation. The subsequent fragmentation achieved with the respective operation determines the cost, throughput and processing requirements for each mining activity. It is one of the aspects that is altered more often and is relatively convenient for adaptation to overcome the limitation of, established, processing plant. Therefore, it has always been under focus for improving the operations in this part of the value chain. For open pit operations it represents an essential value, since the mine goes deeper and steeper with every production cycle, the intent in the production may be to optimize the use of reserves as effectively as possible. (Hustrulid, 1999)

Each ore may require a certain demand in fragmentation to be achieved with blasting, that may be influenced with the plant requirements and cost but, for limestone quarries the usual case for desired fragmentation is to achieve coarse particle size distribution, to avoid as little as possible the material from becoming waste due to the limitation of kilns to not calcine finer particles, under 20 mm. This, as stated before, serves as major concern, since the reserves are not fully utilized, and consequently undervalued production is achieved due to loss of ore. (Singh, 2012)

Studies have been performed in order to optimize this operation but the number of variables determining the final fragmentation are wide in spectrum, therefore, it is difficult to understand the concept.

Current study that is followed looks deep into analyzing the rock mass being blasted along with the parameters that make up each of the blast design. The rock mass under study, exhibits geological features that could be responsible for affecting the mechanism of blast. These features include the discontinuities, fractures, joints and infillings. To classify and give meaning to these features, geo-mechanical classification system, Rock Mass Rating, is used. The use of such system will inherit a distinguished character to each rock mass, thus supporting us in our research and concomitant data collection.

Use of 2D Imaging softwares have been quite popular in overcoming the cost spent in sieving operations by analyzing fragmentation of any blasting operation, showcasing a representative profile for each muck pile. (Aswegen, 1986). Therefore, to support the plan, Each image shall be captured by a drone that shall provide a safer and

comprehensive view of the muck-pile, thus aiding us in our observation; following which the images shall be analyzed for the particle size distribution, in the fragmentation, attained for each blast. The study follows up on this course and presents an outlook for the case present, of Jemelle, to see how this software can be used in an optimized manner along with presenting the use of empirical models for understanding each element that can impact the fragmentation. The test for the model's validity are followed for providing a base for alterations and possibilities, as such, to the current blast design. (Cunningham, 2005).

The study combines the aforementioned elements and provides a comprehensive analysis over the impact and use of the tools. Thus, providing a good source, for following up on regular bases, for understanding and analyzing drilling and blast designs for the respective case; paving way for possibilities to attain an optimized fragmentatin in accordance with the kilns' requirement.

1.1 OBJECTIVE

The objective of the thesis is stated below;

- a) To analyze the drilling and blasting practices at La Bouverie Quarry, Jemelle.
 - a. To study the effect of each of the parameter, of blast design, on fragmentation
 - b. To map the faces of rock benches and see for its impact over the fragmentation
- b) To propose changes to drilling and blast design based on the analysis performed

To achieve the aforementioned tasks, empirical methods shall be used aided by image analysis techniques.

1.2

1.3 SCOPE & LIMITATIONS

The goal of the thesis is to understand the different parameters that characterize each blast. Determination of their respective impact over fragmentation forms major part of the study. Collection of data for each blast performed during the period is necessary, then following up with analyzing each of the blast through comparative studies. The major determinants assumed here along with the blast parameters are the rock mass

characteristics. Each rock mass therefore should be thoroughly analyzed and distinguished with respect to its visible geological features. The study includes the hardness of the rock as a determinant for blast induced fragmentation.

Empirical modelling forms the core of the data collection, as it is being pursued as basis for designing a new blast pattern. Since performing a blast based on intuitive measures may affect the outcome of production and also will impact in understanding the difference in fragmentation profile. The task requires to understand the current practices performed on site, observing their outcome and then follow up with suggestions and recommendations in line with skill level and equipment on site.

The current study performs image analysis using WipFrag; The software is limited with its current version unable to detect fine particle. Even if the images are captured at a lower altitude, distinguishing particles beyond 60mm is quite arduous and difficult. Assumptions shall be followed accordingly in making the software utilization in manner that could support the study and future practices.

The number of blasts analyzed may be limited, in line with requirements of production, that can be affected with demand, maintenance in plant and administrative elements.

Most of the practices such as detection of discontinuities, RQD and analysis of fragmentation involve user biasness, even detection of particles with WipFrag; though the study may be influenced by it, but care has been taken, in order to minimize it by following the practices that are in accordance with literature.

2 LITERATURE REVIEW

2.1 DRILLING AND BLASTING

Blasting make up for an integral part in mining operations. In all hard rock mining operations drilling and blasting are most widely used operational measures for fragmenting or breaking the rock. Each operational activity is pursued in adaptation to the processing demand. As in some mining operations it will be demanded to fragment the material to fine size, so that the operational cost for crushing in a processing plant decrease; while in some cases it may be advantageous to reduce the number of fines generated because the final processing phase may not be adaptable, or the customer needs may require it otherwise.

Blasting is dependent on two major parameters controllable and uncontrollable parameters. Each of the determinants are analysed prior the activity, to minimize error and produce the desire fragmentation.

2.1.1 UNCONTROLLABLE PARAMETERS

The uncontrollable parameters include the geological characteristics of the rock and its concomitant rock mass properties. Both are since in-situ properties of the rock being blasted, therefore, called the uncontrollable parameters.

Geological structures are required to be observed and analysed, mapping of the geological formation can give a good insight how the rock is formed and what quality is the rock. It also gives a adequate information on how the layers of different rocks are aligned, thus, adapting the blast design in accordance with it.

The fractures and discontinuities play an important role during blasting; since blasting requires explosives and the explosive's energy tries to escape from an area of least hinderance therefore every time they encounter a rock with fractures and discontinuities they use these openings to escape. That on one hand, under uses the energy input but on the other hand can be proven advantageous as this process produces fine fragmentation.

Rock Mass properties are well aligned with the geology. It includes the strength of the rock which can respond to blasting energy by either breaking or producing fractures across the rock mass. These artificial discontinuities can have recurring effect in each blast as they are broken and then created again, they have the similar effect like

geological born discontinuities, to create opening for the energy to escape or openings for fine fragmentation.

The shape and structure of each joint and discontinuity impacts the outcome of the blast. According to Hagan, the mechanical and physical properties seems to show a lesser impact over the blast performance compared to the joint and bedding planes. He added that the orientation of joint shall be thoroughly analysed prior blast planning as according to him if the joints are parallel to face then yield shall be higher, as in fragmentation shall be more homogenous. If the angle now is between 30 and 60 degrees, then irregularities shall be observed with the fragmentation. For a case with joints being perpendicular to the face the fragmentation shall not be desirable since the strain energy transmission through block is hindered, this can be overcome by drilling more holes per unit area. (Hagan, 1992)

It is estimated that 55 percent of the blast performance efficiency is determined from the orientation and spacing of discontinuities, therefore assessment of these parameter is essential for optimizing the blast performance. (Ghose, 1988)

Some characteristics that need to be evaluated when it comes to joint and discontinuity assessment apart from orientation are; aperture, which can cause cratering and decrease the quality of the retrieved excavation profile. If the joints are open, then they can also arrest and initiate crack branching between the holes. Too wide spacing can also reflect the explosive energy as the aperture acts as a free face in these conditions. Frequency of discontinuities showcases how intensive are the fractures in the rock. During blast design the holes spacing is adapted to frequency of discontinuities as this may provide with the spacing between adjacent discontinuities.

Joint filling is another aspect, as filling alters the transmission of strain energy, therefore thickness of filling is very important since smaller width may overcome the losses in transmission, but a greater width of filling material may hinder the strain energy transmission thus deteriorating the impact of the blast and resulting in undesirable fragmentation. The type of filling also plays a major role, because let us say; if a clay material is found between the joints as filling, then upon interaction with the explosive energy the clay shall start to swell, resulting in excessive overbreak and underbreak. (Sauvage, 2012)

Lastly, roughness needs to be evaluated as well, to summarize the impact of this property, it can be stated that the greater the roughness the higher the friction force between the joints and greater energy shall be required to overcome and fragment this rock. (Singh, 2007)

The controllable parameters include broadly the geometric parameters, the explosives and the time. Each group shall be discussed as follow;

2.1.2 GEOMETRIC PARAMETERS

Geometric parameters are design characteristics that are assessed and adapted to the rock mass properties and also to the controllable parameters. An inter-relationship between each of the parameters is observed during the design.

2.1.2.1 Drill-Hole Diameter

The drill hole diameter is primary consideration for a blast design. As the other parameters are followed up in accordance with it. Though it must be stated that it is certainly not compulsory to follow the rule of thumbs for other design parameters based on Drill hole diameter but since blasting is a risk driven operation therefore usually it is followed up as stated. Some factors are determinants to selecting the right drill-hole diameter. As the rock mass properties, desired fragmentation the height of the bench, cost and the available equipment.

As mentioned, the determinants play a vital role for selecting the right diameter for the blast hole. Therefore, in depth analysis for this aspect for the case at hand shall be shared in the later chapters. (Zhang X. , 2016)

2.1.2.2 Bench Height

The charge diameter and burden are limited by the bench height. Based upon the working condition and the loading equipment the height of bench is planned accordingly. If the ratio of height to burden is large, it has been found that this will provide ease in displacing and deforming the rock. Certain experimental ratios have been found compared to the type of fragmentation desired. (Ash R. L., 1968)

- When the ratio of height to burden is 1; the fragmentation has been observed to be larger, also producing overbreak/underbreak around the holes and toe of the bench.

- With bench height considered twice as the burden then in that case the size of fragmentation is comparatively reduced and so is the generation of overbreak and underbreak.
- Experience and research has showcased that a ratio of more than 3 between the burden and height can eliminate the abnormalities at the hole and toe, and also may produce a more homogenous fragmentation.
- A very important aspect for bench height needs to be remembered, that increasing the bench height to large values may impact the drilling operations as the drill hole will be prone to higher deviation which may consequently increase the vibrations, generation of flyrocks and overbreak; regardless of the height burden ratio, since it is not easy to keep the explosive consumption constant in this case.

2.1.2.3 Blast-hole Inclination

In order to acquire better fragmentation, avoid excessive subdrilling, improve dissemination of explosive energy from the blast-hole and lower the risk of toe and vibrations; inclination of drill hole is recommended. Though it may alter some aspects negatively since inclination requires expertise from operator and the equipment. Wear and tear is usually observed with excessive inclination practices in blast design. This can also increase the length of the drill-hole, causing greater deviation. Depending upon the requirements and the available resources, it should be well assessed prior to go forward with it in the blast design. (Jimeno, 1995)

2.1.2.4 Stemming

Stemming is performed for each blast-hole to confine the gases inside and avoid the premature escape, which can result in producing flyrocks and airblasts. Excessive stemming can hinder overly confine the blast energy at the lower level of bench, thus generating boulders from the top and elevated levels of vibrations.

The size and type of materials influences the efficiency of blast and the extent of confinement. Research has shown that a diameter ratio of 17:1 between the stemming particle and the drill-hole provides optimum results. Drill cutting can be used as stemming material, due to easier availability but it has been found that crushed rock can be more effective in optimizing the operation of stemming. (Konya, 1990)

Depending upon the quality of rock and the desired fragmentation, studies have shown that the length of stemming column may vary from 25D to 60D. (Jimeno, 1995)

2.1.2.5 Subdrilling

Subdrilling is the drilling beyond the bench height. It is performed to overcome the toe appearance. It may aggravate the level of vibrations produced and increase the cost of drilling, but design parameters may sometime recommend ignoring the cost involved. Ash and Gustafsson suggested subdrilling should be not more than 30 percent of the burden. Hustrulid on the other hand gave a relationship for the subdrilling length to drill-hole diameter, suggesting it to be equal to 8D. (Jimeno, 1995)

2.1.2.6 Burden and Spacing

The distance from the blast hole to the free face is known as burden; whereas the distance between each holes of the same row is called spacing. The value for both the parameters are correlated with the drill hole diameter, bench height and the resulting fragmentation.

Studies and practices have shown that the average burden is designed with size of 20D to 40D. The size of burden is crucial since the hazard of flyrocks and airblast is imminent in small burdens, since the explosive energy escapes and encounters the free face sooner with full zest; whereas large burdens may prove to produce excessive vibrations and lose of explosive energy.

Spacing is usually calculated relative to the burden and drill hole diameter. A crucial aspect while determining spacing is to see the relative difference between the discontinuity spacing and hole spacing. The desired result shall determine the planning in the end. (Zhang X. , 2016) (Rai, 2010)

2.1.2.7 Blast Pattern

The most common pattern followed are the rectangular and square pattern, since the ease with which they can be marked. However, practices have shown that optimum results with respect to efficient use of explosive energy and fragmentation can be achieved by drilling on a grid of equilateral triangles.

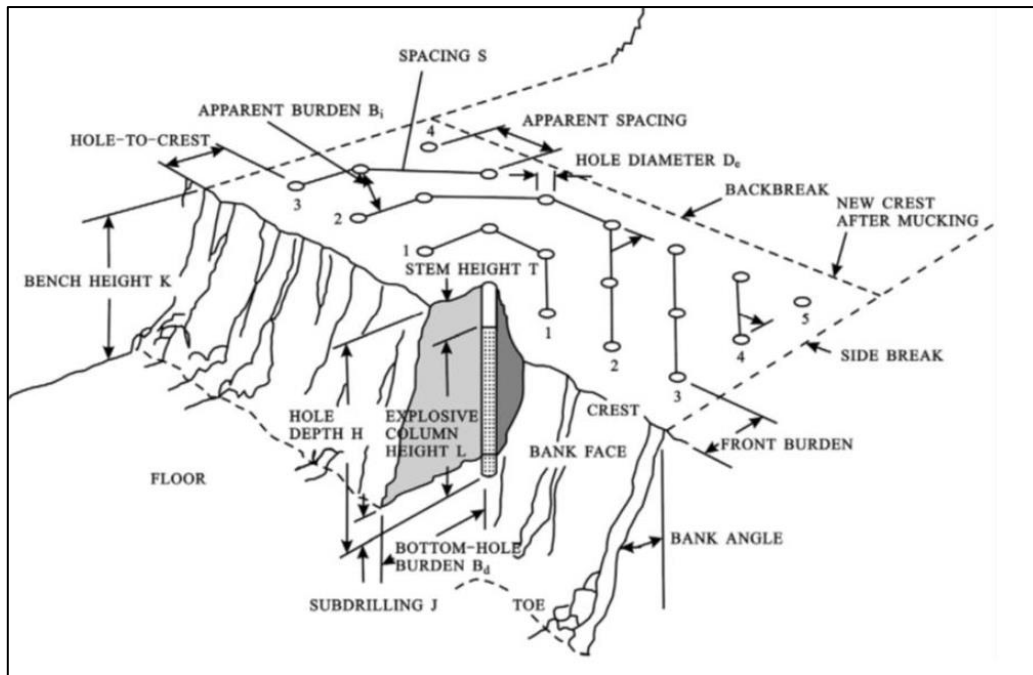


Figure 1; Geometry of Blasting (Ash 1963)

2.1.3 EXPLOSIVES

In order to discuss the characteristics of explosives it is necessary to understand the mechanism with which it causes fragmentation.

2.1.3.1 Blast Mechanism

As the explosive is detonated, a zone is generated that goes down the length of the column at the velocity of detonation, characteristic for each explosive. In front of this zone a pulse of energy known as a shock wave is produced that is transferred to the neighbouring rock. Any space between the explosive or rock will deteriorate the effect as the wave energy would be absorbed in this region.

The energy pulse spreads outward as a compressional wave in every direction at a speed close to the VOD. Depending upon the compressional strength of the rock the transmission causes the rock to fracture and be crushed in proportion to the extent the wave energy is exceeding the strength of the rock. The cracks produced in this scenario are radial as they extend out from the borehole in a radial direction at speed of sound, characteristic for each rock.

As the shock wave reaches the free face, it is reflected due to the bending of the outward compressive forces. Now the wave is converted to a tension wave; though, the speed and energy has been reduced in this transition; therefore, it is usually experienced for open joints where apart from the free face the opening serves as a

free face releasing the energy produced from the explosive. Nevertheless, for the deteriorated tension wave generated, the rock can still break, If the burden is not too large. (Changyou, 2017)

2.1.3.2 Characteristics of Explosives

Following showcase the important properties that need to be assessed prior choosing the explosive for the rock.

2.1.3.3 Detonation Velocity

It is usually expressed as a confined or unconfined value, denoting the speed with which the detonation is carried out inside a borehole or out in the open, respectively. Depending upon the quality of rock, a high VOD explosive would be recommended for a hard rock and vice versa.

2.1.3.4 Density

This property is also associated for explosive with respect to the desired fragmentation. As a dense explosive would be preferred for fine fragmentation in a hard rock. Also, the condition of groundwater in the borehole may determine the need to assess the density of the explosive, since usually the density for explosives ranges from 0.7 to 1.7 g/cm, therefore one with density higher than 1 should be chosen if the borehole contains water.

2.1.3.5 Detonation Pressure

A property determined from the VOD and density of the explosive denotes the pressure exerted by the shock wave produced. As mentioned earlier, the energy is reduced upon release and encountering gaps and faces therefore care should be taken by accommodating the loss as tolerance for each blast performance. (Cooper, 1996)

2.1.3.6 Water Resistance

It is the measure of the ability for each explosive to resist a degradation in its sensitivity, as its exposed to water. The ease with which detonation takes place is known as sensitivity.

2.1.3.7 Fume Class

It is one of the safety character for choosing the right explosive. As each explosive produces undesirable gases such as CO and NO_x. The fume class denotes the quantity of these poisonous gases being produced. Depending upon the standard followed for each country ratings should be assessed, in order to avoid exposure to hazardous gases in post blasting atmosphere.

2.1.3.8 Delay

The time parameter is distinguished in two types the delay between holes and the delay between rows. A consensus, over the years, have been reached determining 3ms/m of delay for maximum fragmentation. Though that may not be desired in every case therefore, adaptability to each scenario shall be established with practice. A data in the figure is shared showcasing the factor that fragmentation increase up to 3ms/m of burden and then worsens gradually. Excessive delay between holes is not recommended if the desire is to increase fragmentation.

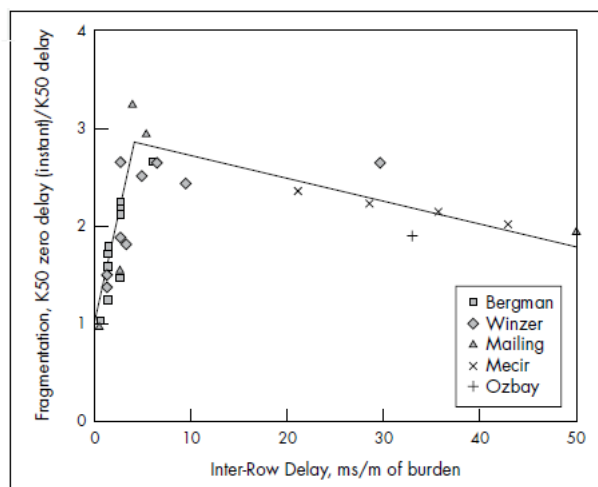


Figure 2 Effect of hole-to-hole delay on fragmentation (SME, 2011)

Insufficient delay is not recommended either as it may generate excessive throw, as well as back break and over break. When the two neighbouring holes fire together this results in the rock between them to split and generate a premature propulsion, giving poor fragmentation. The sudden reduction in fragmentation is observed because the energy is used in the throw. (Rai, 2010)

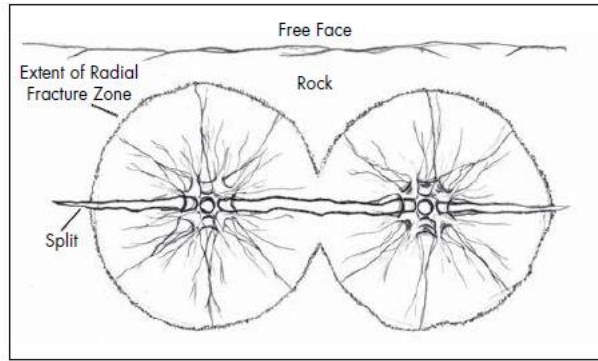


Figure 3 Effect of simultaneously fired holes splitting at S/B ratio of less than 2:1; (fracture face coalesces and provide a split before fracturing reaches the free face) (SME, 2011)

Similarly, for the row to row delay, care should be taken to overcome back break and result desired fragmentation.

2.2 FRAGMENTATION MODEL

A variety of models have been brought forward to aide in estimating and preparing an optimistic blast model with desired fragmentation. Two approaches have been recorded to design each plan for blasting.

- Empirical Modelling
- Mechanistic Modelling

Mechanistic modelling accommodates each aspect of the blast design as it provides intrinsic information on the effect of the parameters chosen to determine fragmentation. However, application of such modelling is an uphill task with respect to cost, time and data collection. Besides the empiricism is involved in this modelling to some degree, which may reduce the accuracy for the subjected task. (Cunningham, 2005)

Empirical models are therefore used, by operational team, instead; to determine the effect and predict the fragmentation produced from each blasted design. The model most popularly used these days is Kuz-Ram model, since its inception in 1983; it has been updated and improved over the years to accommodate the development of blast design with respect to the parameters introduced. (Cunningham, 1983)

2.2.1.1 Kuz-Ram Model

As mentioned, the model was proposed in 1983 at a conference in Lulea. The model makes use of three parameters;

- mean fragment size, X_{50} , calculated by using Kuznetsov equation

$$X_m = AK^{-0,8}Q^{\frac{1}{6}}\left(\frac{115}{RWS}\right)^{\frac{19}{20}}$$

Where, A = Rock Factor; K = Powder Factor (kg/m^3); Q = Mass of Explosive/hole (Kg); RWS = Relative Weight Strength (Explosive Property relative to ANFO)

- Factor for Sieve size, denoting the % of particles passing a certain sieve size. This parameter is calculated using the Rossin-Rammler equation. The parameter can also be used in determination of size distribution for a muck pile

$$R_x = \exp\left[-0,693\left(\frac{X}{X_m}\right)^n\right]$$

Where, X_m = mean particle size (cm); X = Screen opening (cm)

- Uniformity index 'n'; a parameter that takes into account each of the blast parameter. Through excessive investigation by Cunningham he proposed the following equation.

$$n = \left(2,2 - \frac{14B}{d}\right) \sqrt{\left(\frac{1 - \frac{S}{B}}{2}\right) \left(1 - \frac{W}{B}\right) \frac{L}{H}}$$

Where, B = Burden (m); d = drill-hole diameter (mm); S = Spacing (m); W = Drill-hole deviation (m); L = drill-hole length (m); H = Bench height (m)

As it can be deduced from the equation that not all the parameters were considered in the model proposed by Cunningham. Therefore, with the advent of time, additions and editing to the model were carried out. As important variables were introduced into the modelling calculation, including the timing and delay between holes and its precision and the properties of the rock and its amassed structure. (Adebola, 2016)

Following final equation was proposed for the uniformity index calculation.

$$n = \left(2,2 - \frac{14B}{d}\right) \sqrt{\left(\frac{1 - \frac{S}{B}}{2}\right) \left(1 - \frac{W}{B}\right) \left(\text{abs}\left(\frac{BCL - CCL}{L}\right) + 0,1\right)^{0,1} \frac{L}{H}}$$

Where, BCL = Bottom Charge Length (m); CCL = Column Charge Length (m).

As a supporting tool in the model validation, KCO Model would be used just to see the difference between estimation of fine particles, which Kuz-Ram is infamous for underestimation of this region. (Souza, 2018) The difference is using an undulation parameter, factor multiplied with the uniformity index and also instead of Rossin Rammler equation a new equation is used for calculating the material passing a certain sieve size $P(x)$;

$$P(x) = \frac{1}{1 + \left(\frac{\ln \frac{X_{max}}{X}}{\ln \frac{X_{max}}{X_{50}}}\right)^b}$$

Where, X_{max} is maximum particle size(cm), equivalent to spacing and burden.

$$b = [2 \ln 2 \ln \frac{X_{max}}{X_{50}}]n$$

2.3 IMAGE ANALYSIS

With increasing demand of minerals, day to day advancements and developments, have proceeded to engage the customers by maintaining the supply. Data storage has been one of the aspects that has led the mining industry to follow the trend. As the industry tries to adapt to safer and time effective strategies by imaging the outcomes of each of the activities and then after analyses, optimizing the operations. Imaging provides the opportunity for data storage as well as changes in operation in line with optimization and can be correlated with previous data pictures and relative gain can be known. Besides Image analysis method provides advantageous approach than sieving. Since the method is non-destructive all sorts of rocks can be analyzed; It is quick, and analyses can be performed rightly fast as well. The method also provides the opportunity to continue analyses without hindering the operations. It also gets the upper hand for being able to analyze several samples that could reduce the error significantly. (Maerz, 1996) (Pong, 1983)

The inception of image analysis in mining was brought forward for the blasting operations. As the muck pile was photographed by superimposing a grid over it, the conclusion from the experiment was that the assumption of considering the surface distribution as representative is rather (Porter, 1974). Later on, experiments were performed over industrial mucking by taking samples into laboratory and analyzing the

photographs with superimposed grid; with concluding remarks of having inadequate resolution for studying the correlation between the grid and the particle size. (Bonneville, 1980)

The research for adopting image analysis continued in the later years as Borg et al took various photographing methods available at the time and reviewed their outcome for evaluation of fragmentation. (Borg, 1983) The conclusion was that the methods are time consuming and requires extensive manual input. Therefore, a few images were taken as study samples for representation for the complete profile. Secondly it was added that the bias of overestimating coarse particles and underestimating fines also hinders the approach to be progressive. Carlsson and Nyberg, in the same year, put up a set up that involved an online TV camera for acquisition of image, followed it by digitizing and evaluating the image using a microcomputer and the result could be then printed via a printer. The set up was promising, as it involved the study and use of edge detection techniques to measure the area of particles, the area could then be made source for determining the volumetric size distribution, but due to limitation of processing power and memory of the computer in those times the project could not give out its intended results as it was limited to the use of chord length method for making the calculations simpler.

In 1987, a system was incubated at the University of Waterloo, called WipFrag, that was capable delineating the fragments manually and was able to extract the particle edges, hence called a semi-automatic photoanalysis method. The system was later commercialized in 1995 (See next topic).

Continuous advancement in technology, furthermore strengthened the interest in the area as more opportunities started to appear. As the system, initially being used for analyzing blasting fragmentation, was now extended to mineral processing operations. (Maerz N. , 1999)

It has been argued that performing the analyses using 2D measurements can encounter errors, as it varies due to color, texture, light and shade, the time and the angle with which the picture is taken etc. (Thurley, 2002) Therefore, implementation of 3D surface data was taken up and deduced that the data surfacing from the system is independent from the outside factors that decrease the credibility of 2D measurement. The system then on generated were able to distinguish between a

partially or entirely visible particles. Over time improvements have made it a sought-out system as development in morphological processing techniques made it able for it to be applied in ship loading (Anderson, 2010) and move further on to real time measurement of particle size distribution for limestone. (Thurley, 2011)

On reviewing the study, it can be concluded that 2D measurements have been well integrated in the industry and 3D measurements are on verge of becoming a common name. But the atmosphere in reality for any operation is hindered by the process and by the cost of the process; so on the base of this thought considering a combination based on correlation of data between the two techniques may prove advantageous.

2.3.1.1 WIPFRAG

As mentioned earlier, the system was a breakthrough in its time and has achieved great recognition across the industry for analyzing the fragmentation post-blasting and during comminution stages in the processing plant.

Its input for the software can be recovered from roving camcorders, fixed cameras, digital files and lately UAVs imaging. It uses the algorithms that can automatically detect the individual blocks and outline them based on the edge detection parameters, that include thresholding and various gradient operators. Furthermore, manual drawing and input can improve the detection and outlining procedure, because the input of image quality serves as a main determinant for the result. Therefore, care should be taken, while using images for the program. As the program is sensitive to the lighting, distortion and quality of the image certain pre-requisites are advised to be followed; (Leite, 2018)

- To capture the image perpendicular to the pile.
- The strategy for imaging shall be kept consistent, to overcome any correlation error.
- No particle, photographed, shall cover more than 20% of the picture.
- The optical distortion shall be reduced by keeping the imaging overlap at 80%.
- The time for imaging, environmental conditions, weather shall all be considered prior performing the test. Homogeneity in the method is key to optimistic results.

Various mining operations have practiced and made significant leaps in optimizing their operational outcome. As INCO Coleman Mine managed to reduce their cost by up to 80% as they expanded their blast pattern. They managed to retrieve data

regarding the coarse rocks being produced due to each blast, the statistical data acquired via the program gave them a good idea over their approach as they kept on altering their blasting pattern and then correlating the results with the fragmentation histogram to see the effects. Each expansion showed a reduction in the coarse generation, ending in giving them the aforementioned savings.

Similarly, Selbaie Mine in Canada was able to graph the details in the complete value chain of mining as the fragmentation data obtained from WipFrag was used to estimate the cost in processing, rate of loading and hauling and in characterization of rocks across the mine. The data collected was evaluated and optimization in procedure was adapted to demands.

Several other cases have been reported and published, that made use of the program and acquired significant results for optimization of their processes. (Maerz T. C., 1999)

2.4 UAVS IN MINING

The mining industry lags none, as transition to advanced technological practices are performed across the globe. Considering the risks and hazards involved in the industry operations, It is prioritized in each aspect to practice safety. Such has been brought forward by Unmanned Aerial Vehicles (UAV) or popularly known as drones. Though a name more familiar for defence industry but lately the equipment has revolutionized the surveying, monitoring and volume calculation tasks in mining industry. But the advantage for the equipment is far beyond the current practices. Imaging of the fragmentation can be performed without risking a health hazard of fall, slip or slide on the pile or from the bench. The 2D and 3D image software have made it popular for companies to take in these equipment and perform imaging at desired angle and height. Certain practices need to be undertaken in order to optimize the use of the UAVs. (Bamford, 2017)

An important aspect to be taken in consideration with Drones is the Ground Sample distance. It is the distance represents the real-world measurements into equivalent pixels, e.g. in an image width with 2400 pixels, with the real-world length of the image may give 50 meters, then GSD would be 20,83/pixel. A deduction from this can be, the smaller the GSD the higher the resolution. The GSD for any image may vary because it depends upon the sensor width of the camera, focal length and the height at which the drone was flying above the object or surface to be mapped. (Dering, 2019)

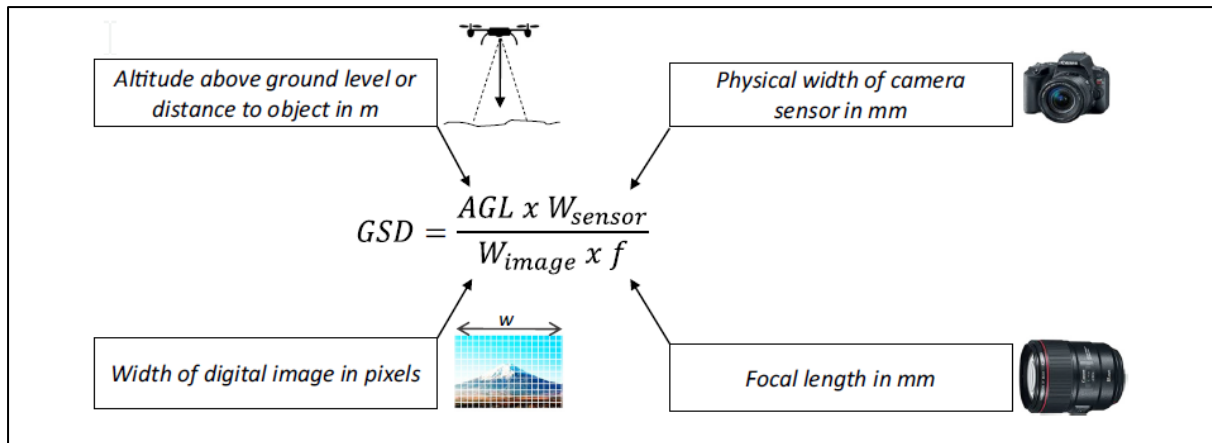


Figure 4 Measurement of Ground Sample Distance (Dering, 2019)

It has been becoming a common practice for using mission planned software to operate the UAVs. The software allows to plan and task the drone to fly on a predetermined path and image along the way, thus allowing a more accurate base for covering a certain zone, being mapped.

Some practices to follow for imaging fragmentation or mapping in mines with UAVs are following;

- Line of sight of Drones is recommended at all times, better to fly during daylight hours
- Flight regulations and constraints should be regarded prior using at certain altitudes
- Imaging at altitudes between 30-60 m has been regarded to be optimal for fragmentation imaging
- Flights are preferred to be +/- 2 hours of noon, due to lighting
- Depending upon the area, try to capture as many images as possible for better results
- Avoid flying in closed areas or too close to structures or benches
- Analyse the weather condition prior flight, drones are sensitive to rain, heat and wind
- Respect the privacy of individuals, during flight, proper channel and permission is mandatory for each flight. (Leite, 2018)

3 INDUSTRIAL CASE

3.1 JEMELLE SITE

Jemelle is a town located near Rochefort in the province of Namur, Walloon region, Belgium. The production site has been in operation since 1924, recent statistics dictate that it employs 468 people directly and indirectly. The plant is producing around 400000 tons annually of lime, majorly for the steel producing customers.

Jemelle site is divided into two parts;

- Quarry
- Plant
 - Limestone Preparation Plant
 - Lime Kilns

The plant and quarry both operate in two eight hour shifts from 0600-2200. The limestone extracted from the quarry is fed into the processing plant which is further processed there to be conveyed into the kilns for lime production. Of the 1,8 million tonnes of limestone extracted 27% goes into producing aggregates while the remaining 73% is utilized for lime production.

3.1.1 GEOLOGY

The quarry is located 3 km north of Rochefort on the Gerni plateau at the south eastern border of Dinant Synclitorium, covering an area close to 60 hectares.

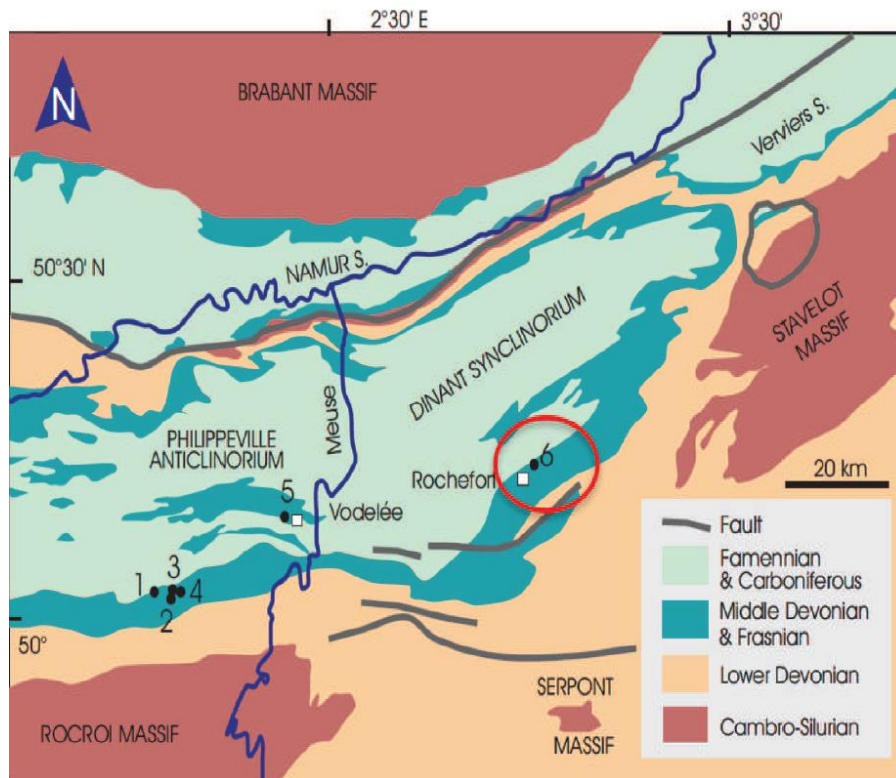


Figure 5 Geological map of southern Belgium showing main Frasnian buildups, where La Boverie quarry is represented by number 6 encircled in red (Boulvain et al., 2005)

Earlier studies suggested that the Frasnian of the Dinant Synclinorium constituted carbonate mounds divided in three types. In increasing order of age, Petit-Mont, the Lion and the Arche were identified then. Later studies revealed the recognition of an additional member called La Boverie, located between the Arche and a member called Beiumont forming the base of Lion. The Lion and Arche constitute majorly of carbonate buildups.

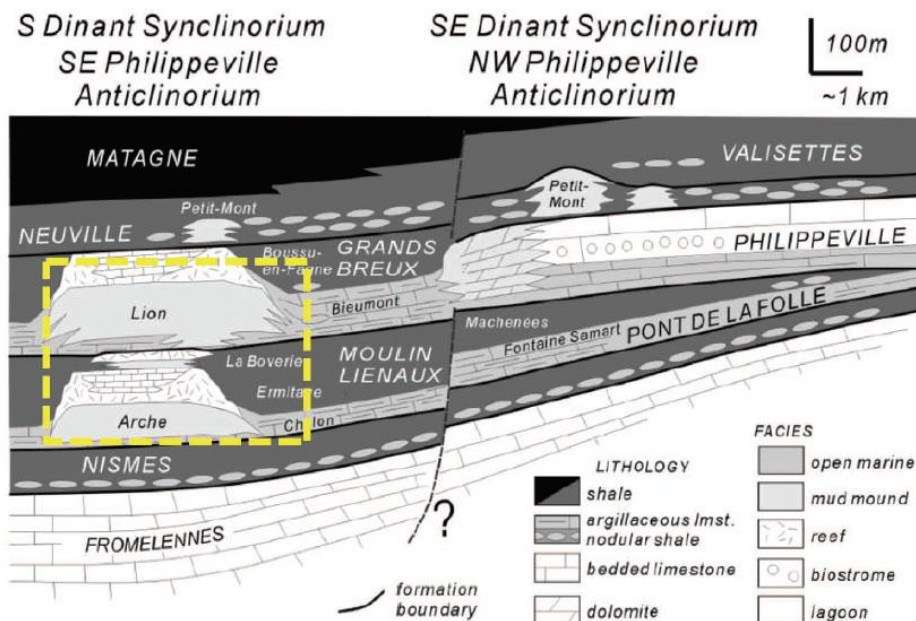


Figure 6 S-N cross-section and lithostratigraphic subdivisions of the Frasnian of the Dinant Synclinorium (Boulvain and Coen-Aubert, 2006)

As marked in the image, the La Boveries quarry intersects a region of 1.1 km of the total 3.5 km (approx.). The quarry as shown lies in the Moulin-Lieaux and Grands-Breux formation. The Lion and Arche both constitute bedded limestone at top and argillaceous limestone with nodular shale at bottom. For characterization of La Boverie member, presence of shale is major constituent.

A detail study was performed by Boulvain and his colleagues, distinguishing each of the carbonate mounds on the basis of the organic assemblages and texture range. Table 1 holds a summary of the division. (Coen-Aubert et al, 2006) (Boulvain et al, 2005)

Table 1 Description of the six build facies and three flanking facies defined by Boulvain et al., 2005

No	Name of Facie	Type	Description
1	A3 & L3	Buildup facies	Grey, pinkish or greenish limestone with stromatactis, corals and stromatoporoids
2	A4 & L4	Buildup facies	Grey limestone with corals, peloids and Udotaeacea

3	A5 & L5	Buildup facies	Grey microbial limestone
4	A6 & L6	Buildup facies	Grey limestone with dendroid stomatoporoids
5	A7 & L7	Buildup facies	Grey laminar fenestral limestone
6	A8 & L8	Buildup facies	Bioturbated grey limestone
7	b	Flanking facies	Microbioclastic packtones
8	B	Flanking facies	Bioclastic packstones and grainstones
9	L	Flanking facies	Packstones and grainstones with peloids and lithoclasts

Based on the sections a model was developed by the aforementioned researchers. As shown in the Figure 7.

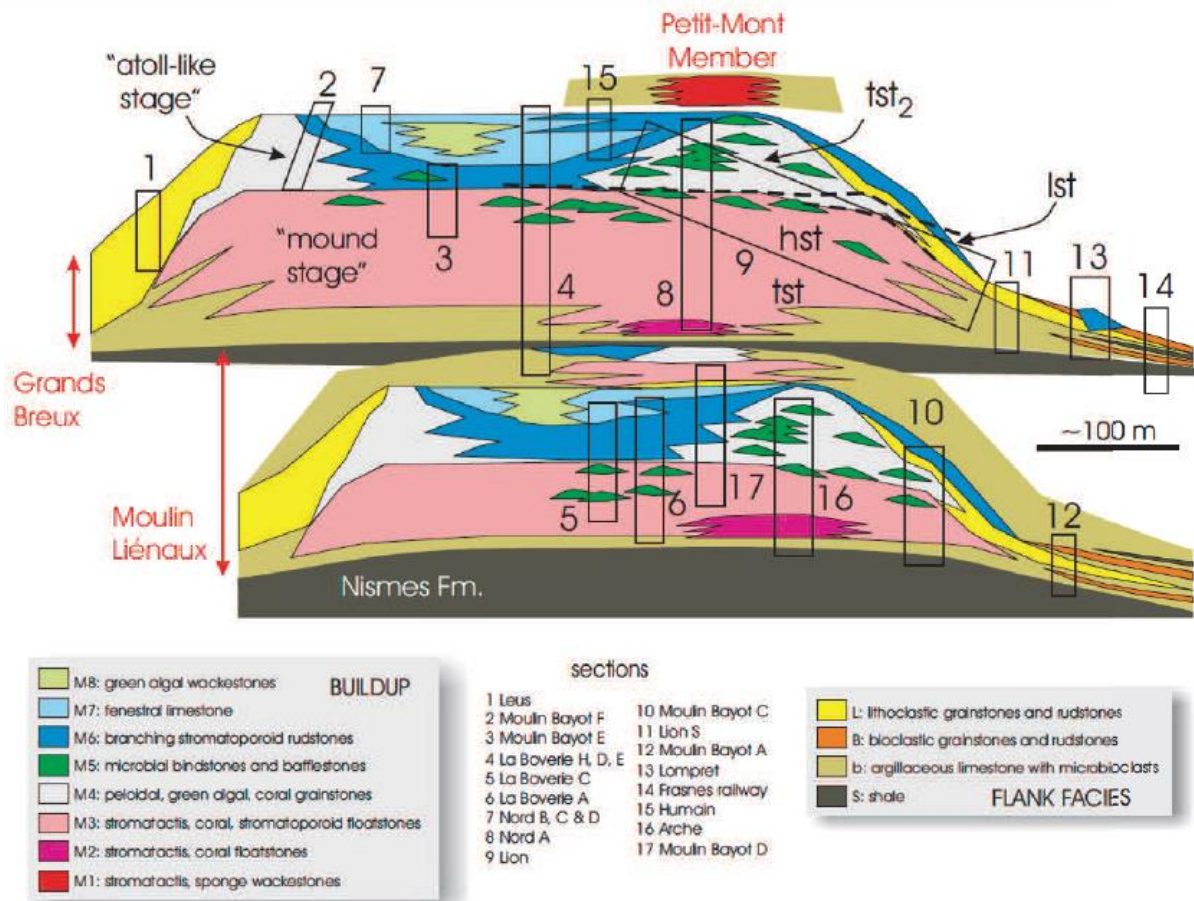


Figure 7 Sedimentological model by Boulvain et al., 2005

As can be seen in the figure, that section 4, 5 and 6 denote the La Boverie region. A cross sectional view has been prepared for self-understanding by the company, distinguishing the members and also showcasing sub-vertical faults in the South east, parallel to the layers.

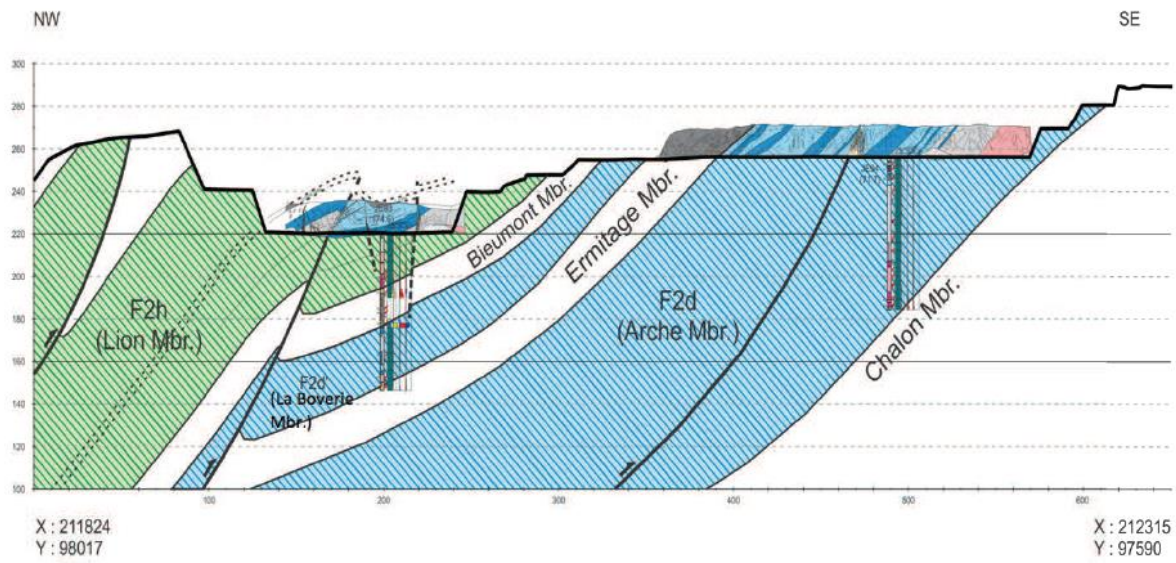


Figure 8 A NW-SE cross-section map of the La Boverie quarry representing the carbonate mounds (Lhoist S.A.) In the quarry and each of the zone are named as F2D, F2H and F2D', representing Arche, Lion and La boverie member respectively. For Lime production, stone is extracted from the F2D and F2H region while due to high shale content of F2D', the stone from this region is used for aggregate production.



Figure 9 A cross-sectional view of the exposed mining faces from La Boverie quarry representing the three units, the measurement of scale is approximate.

3.1.2 LIME PROCESSING PLANT

The run of mine, post blasting is hauled into the preparation plant. Where, the stones undergo crushing in two stages, to adapt to the size requirement for the feed of kilns. As showcased in the flowsheet, the crushed stone is separated in five fractions; 0-4 mm, 4-20, 20-40, 40-80, 80- 120mm.

Stone preparation in the plant begins with the run of mine unloaded onto the apron feeder that feeds the Jaw crusher. The 0-1000mm stone from the blast is separated upfront; as a rotary scalper separates the stone under 120mm and sends the remaining ahead into the jaws for crushing. The equipment installation aids in avoiding over crushing of such stone and has been attributed to increasing the effective through put of the process.

Post crushing the stone, 0-300mm is conveyed onto a deck screen, where it is classified in to fractions of 0-60, 60-120 and 120 to 300. The latter is processed further by being fed into the secondary crusher which is a Roll crusher of the capacity 600 tph. Here the stone is crushed to the desired fragmentation size of under 120mm. The proceedings from the secondary crusher is furthermore classified again, and along with the 60-120 is conveyed onto the respective stockpile with particle size fractions of 40-80, 80-120. Which are then fed into the kilns. The earlier scalped 0-120 is conveyed along with the left fractions of 0-40 and 0-60 to the washing plant to remove the slimes and unwanted residual material. This residue majorly constitutes, clay or fine calcites.

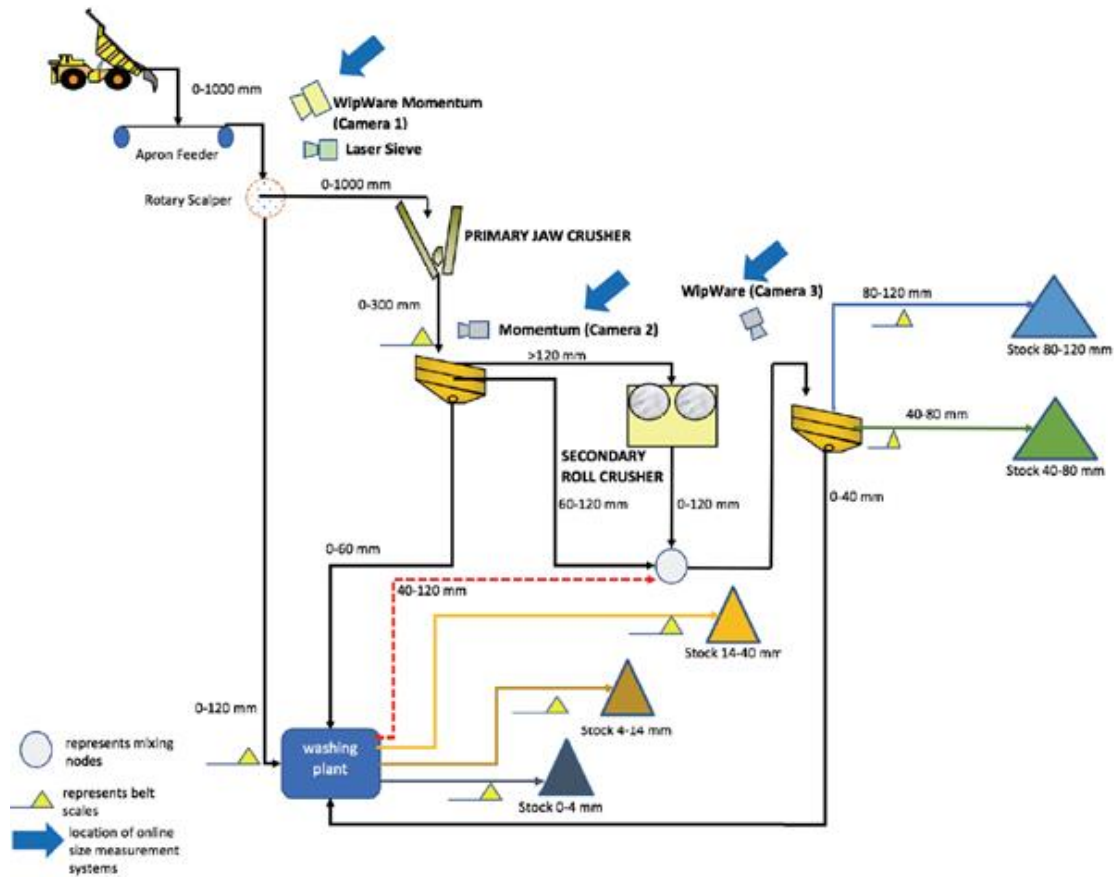


Figure 10 Processing Plant Flow Diagram – Jemelle (Lhoist S.A.)

The washing plant is an integral part of the complete process cycle. As mentioned the residual impurities are removed in this segment from the material that is under 120 mm.

The feed for the washing plant constitutes the Run of Mine that was scalped, -120mm, prior entering the jaw crusher. The fraction -60mm is retrieved from the double deck screens, post primary crushing unit. Lastly the -40mm is classified by the deck screen, installed after the secondary crusher.

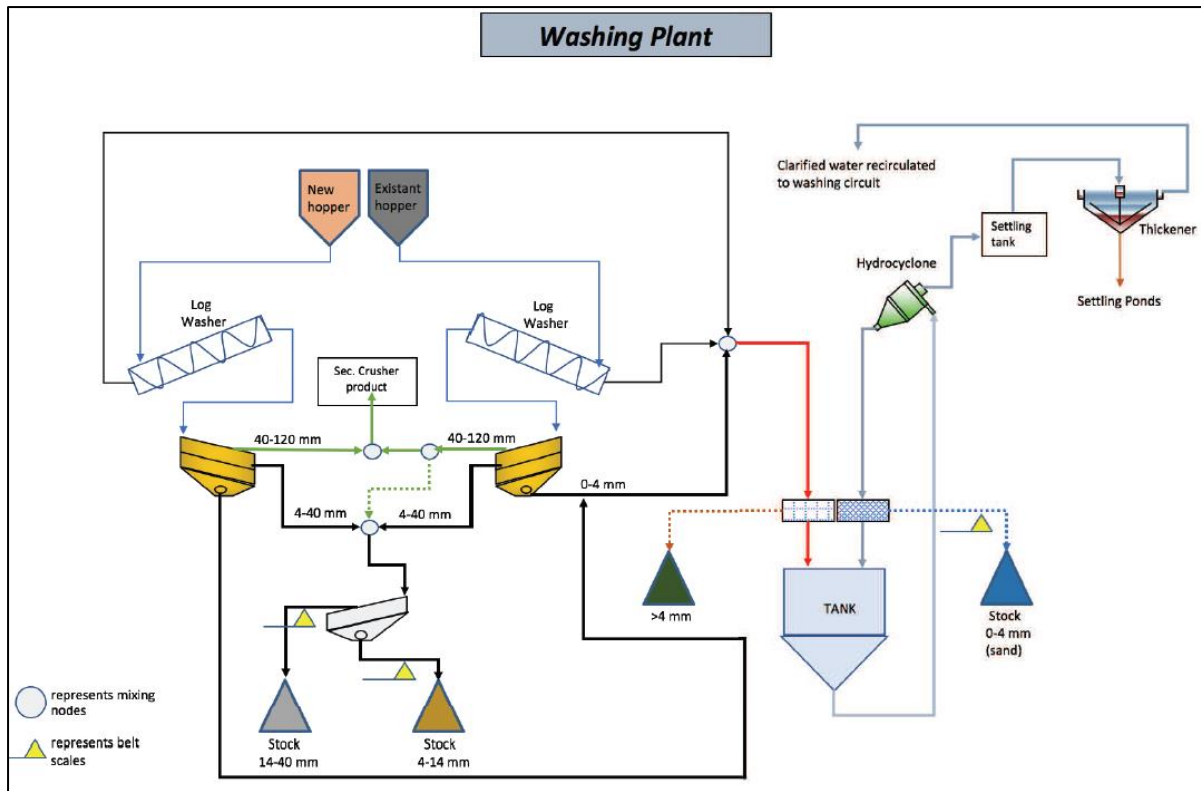


Figure 11 Washing Plant Flow Diagram (Lhoist S.A.)

An overview of the plant process can be seen in the flowsheet. As showcased, the material is fed via two hoppers. with extended streams that go through a log washer, falling from there onto double deck screens that classify the material into fractions of 0-4, 4-40, 40-120mm. The latter product is recirculated back on towards the stone preparation plant, where it combines with the product from the secondary crusher. The fraction of 4-40 mm is separated into two further fractions 4-14 and 14-40mm. The material of the size 0-4mm is conveyed to the hydro-cyclone; the overflow is passed through a thickener from where the water is recovered; recycled for the washing plant and the sediment is sent to tailings pond. The underflow, on the other hand, is sent back onto a desliming screen from where 0-4mm is recovered.

3.1.3 KILNS

For the production of lime, two types of kiln are installed at the plant. Maerz and Annular shaft kiln. The number of units in total is six, of which 5 are Annular shaft kilns and one is Maerz. Table 1 show feed range and capacity for the aforementioned kilns.

Table 2 Kiln feed and Capacity details

Type	Number of Units	Feed Size Range	Capacity (tonnes/day)
Maerz Kiln	1	40-80mm & 80-120 mm	650
Annular Shaft Kiln	3	40-80 mm	140
Annular Shaft Kiln	2	20-40 mm	140

3.1.3.1 Maerz Kiln

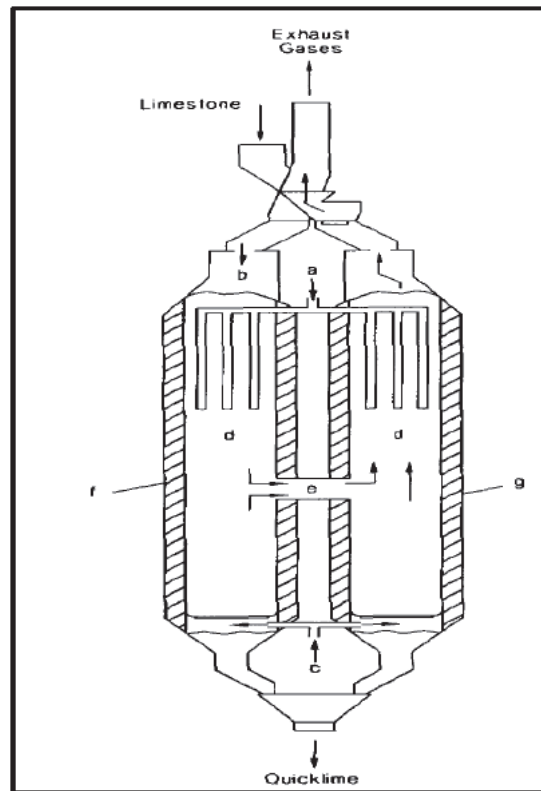


Figure 12 Schematic diagram of a parallel flow regenerative Maerz kiln where (a) fuel; (b) combustion air; (c) cooling air; (d) kiln gases; (e) air duct; (f) shaft 1; (g) shaft 2 (Oates, 2008)

A high capacity and efficient kiln; accepted well in the lime industry. In the schematic you can see that, it constitutes of two vertical shafts connected with each other. The feed is against the orientation of shafts and undergoes three processes, distinguished as zones.

- Preheating Zone: In this zone the feed is initially dried and then preheated to calcination temperature.
- Calcination Zone: Also known as the burning zone; here the limestone dissociates itself to quicklime
- Cooling Zone: Finally, the quicklime produced through dissociation is then cooled.

There are two stages involved, each stage lasts between 8 and 15 minutes. In the first stage, shaft 1 is involved here the fuel is injected which burns eventually in the presence of the combustion gases blown in the downward direction. The heat from the burning is utilized for the dissociation of Limestone (Calcination) the lime produced post this process is then cooled by the air blown upwards, as can be seen in the schematic. The carbon dioxide and the air from combustion and the cooling, all are diffused via an inlet into the second shaft. Here these gases collectively flow against the burden to heat the feed that is still in the preheating zone. From there on, it is then vented out from the top. Hence the recirculation and reuse of the heat proves to minimize the use of energy, which is what makes the Maerz so popular. An added advantage of using this kiln is the minimization of the risk of overheating the lime because of the flow and the movement in the calcination zone.

The second stage is same as the first but this time the roll is reversed between the shafts. As now the fuel and air enter into the second shaft and from there onwards undergo the same procedure of heating cooling and then discharging the waste and air to the neighboring shaft, from where similarly the gases, post heating the feed in the preheating zone, are discharged from the top.

The maerz kiln at Jemelle is fired with pulverized lignite and air.

3.1.3.2 Annular Shaft Kiln

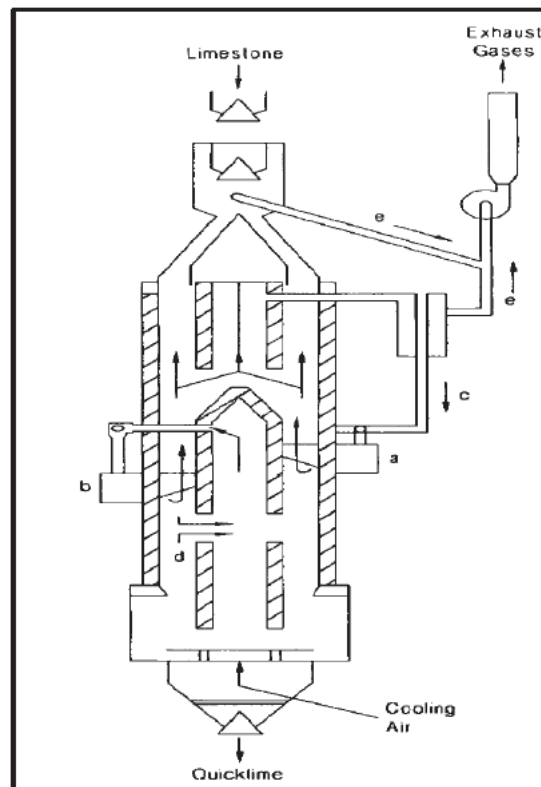


Figure 13 Annular shaft kiln where (a) upper burners; (b) lower burners; (c) combustion air to upper burners; (d) combustion air to lower burners (e) kiln exhaust gases (Oates, 2008)

As can be seen in the schematic, the feed is charged from the top and headed down through the annulus, located between the walls and the central cylinder. The charge passes a similar zonal cycle Maerz kiln, preheating, burning and then cooling. After passing the cooling zone the feed is discharged as product from the bottom. Two burners are used for heating, the primary burners known as the upper burner majorly provides the heat through burning of fuel, the secondary burner aides in supplying oxygen for effective fuel combustion. A characteristic central cylinder plays a vital role in maintaining the burden thickness and distribution of heat across the feed bed. It also helps by pushing the air down and allowing it to mix with the cooling air, which consequently decreases the temperature of the flame ensuring a low temperature calcination process which subsequently gives a low residue of carbonate. (Oates, 1998)

3.2 CASE FOR JEMELLE

As showcased earlier with the flow sheet, the plant produces the following fractions that become feed for the kilns

- 0-20 mm
- 20-40 mm
- 40-80 mm
- 80-120 mm

The particles under 20 mm are not able to be valorized with the kilns therefore their generation in production needs to be minimized. Secondly the particles between 20-40 mm can be valorized but the efficiency of the annular shaft kilns to calcine them is very low. Therefore, it is expected to reduce the fraction of all particles under 40 mm.

To understand the problem, it is to be understood that 50% of the stones in the total production fraction (0-120mm) are directly coming from the blast. Among these fractions the current issue with production is that, of the total, major proportion of the blasted fraction is in the finer region, as can be seen in the Table 3. The table shows the fraction of 50% of final production that is assumed to be coming directly from blast in the stated size range.

Table 3 Blast Fragmentation Fraction, by back calculation from total production (Materne, 2018)

Particle Size	%Total
0-40 mm	66,4%
40-80 mm	13,78%
80-120 mm	19,82%

This fraction needs to be minimized if the feed for kiln is to be increased. Therefore, the objective is followed up with an approach to see the aspects of the blast that are cause for the generation of such high proportion of fine particles.

4 THEORETICAL APPROACH

4.1 PURPOSE AND METHODOLOGY

Prior to implementing any changes to blast design. A thorough theoretical study was necessary. The study involved the aforementioned Kuz-Ram model. Using the model, each of the parameters were analysed and plotted to produce the designated fragmentation particle size distribution.

A reference bench was taken whose rock mass was initially mapped using ImageJ. The mapping involved distinguishing each of the discontinuities, their profile with reference to length, spacing, filling roughness. Using the data from mapping, a geochemical classification system known as Rock Mass Rating was used for classifying the rock (Bieniawski, 1976). The bench face was divided into Zones with each zone being treated different with reference to the RMR properties, initially. Then a combine average of total is used for classifying in the end to showcase the relationship. This should be borne in mind that while practical examination is followed, each zone will be treated separately for determining the impact of blast design for that respective zone. This can be understood in this way, as if the rock mass is weak and fractured excessively, considering the powder factor and drilling conditions to be the same then it will be fragmented relatively more than an intact zone. (Choudhary et al, 2013)

The quantity of explosives will be kept consistent for determining the reference point, this data was retrieved based on the previous blast performed in the reference zone. Based on this point, changes will be performed in altering the quantity in total. Though the type of explosives shall not be changed citing availability and feasibility due to vendor customer contracting complications. However, as mentioned, alteration to the quantity will be considered, as in, it will be interesting to see the changes in Explosive energy upon the fragmentation, which will require changes to the quantity of each of the three-explosive media used.

Following parameters shall be quantified with their relative fragmentation performance.

- Burden
- Spacing
- Drill hole diameter

- Specific Explosive Energy
- Powder Factor
- Bench Height

The model shall be formulated for both type of benches, F2H and F2D.

This has to be noted each time one of the parameter is altered the rest are kept as in the base case, base case parameters are from a usual blast performed on the respective bench.

4.2 RESULTS AND DISCUSSION

4.2.1 SENSITIVITY ANALYSIS

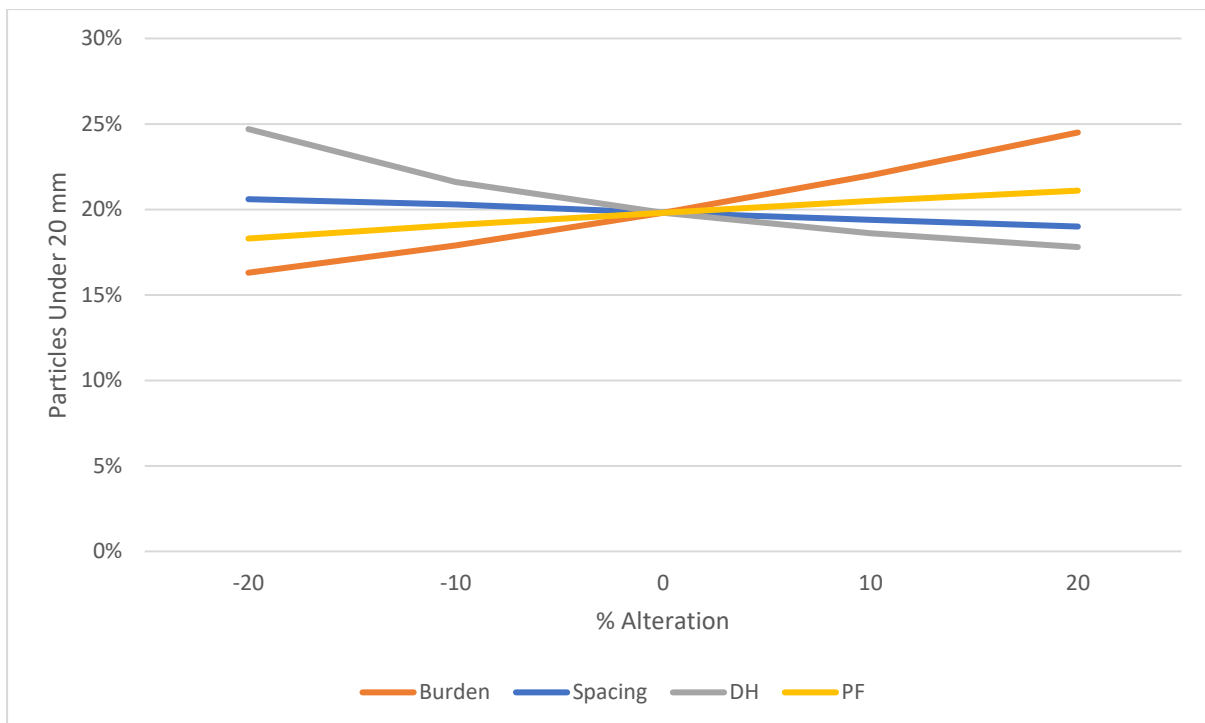


Figure 14 Sensativity Analysis for Different Paramters

A sensitivity analysis was performed showcasing the change in Drill-hole diameter, burden, spacing and powder factor. These parameters, each was altered with respective %amount.

4.2.2 BURDEN

For the changes in burden, it can be deduced that with raising the length of burden we experience a coarser fragmentation and vice versa. This is because, as the burden increases, the explosive energy scattered from the borehole is attenuated along the way, by the rock mass. This attenuation of energy causes the rocks to break and be

fractured. Therefore, once it reaches the free face and is reflected as a tensile force it is easier for the, now, weak energy to fragment the excessively fractured rock. Similarly, by reducing the burden length, a decrease in fine generation is observed, because, now, the explosive energy reaches the free face sooner and loses its potential and opportunity of weakening the rock mass by fracturing it. (Vedala, 1987)

4.2.3 SPACING

An opposite trend is observed for the changes to spacing between drill-holes. Relatively, the change in fine generation is less as well. This is because the initial spacing was comparatively less to burden quantity therefore the %change was consequently less as well. Regardless, the increase in fines with decreasing spacing is because, firstly, each drill hole is being detonated with a delay between them so each experiences the explosive energy fragmenting the zone nearby and as the explosive energy starts to scatter the nearer the neighbouring drill-hole the more the rock experiences the energy in that area, hence fracturing relatively more than usual and the same phenomenon follows, as the reflected shockwave from the free face finds it easy to break this rock in fragments. (Kecojevic et al, 2007)

4.2.4 POWDER FACTOR

Powder factor is the amount of explosive used in breaking one tonne or one m³ of rock mass. It can be easily understood if we increase the powder factor that means we are increasing the explosives. By increasing the explosives, we are consequently enhancing the force of the shockwave hence more fragmentation and for our case fine fragmentation is obvious.

4.2.5 DRILL-HOLE DIAMETER

As mentioned earlier, drilling diameter is the basis upon which blast models are designed. But for now, as our consideration is merely hypothetical, it is not constrained by practice neither by the cost. As it can be observed from the graph that increasing the borehole diameter will reduce the fine particles. This can be understood by the reason that by increasing the diameter we are decreasing the charge length since ANFO is added as bulk then assuming that it is confined perfectly in the hole, then by increasing the diameter we are decreasing the length it is added. This increases the stemming and so forth, one gives an invariable fragmentation distribution and secondly increase the coarse size particles. By decreasing the drill hole diameter vice versa, we

have more fine particles. It is also experienced that smaller diameter holes require smaller spacing between the holes, so that the blast is effective in fragmenting the rock. This further ensues with increase in the number of holes being drilled in a certain size bench, thus increasing the cost.

Another element that the model does not take into consideration is the shock wave generated. If we decrease the diameter of the blast-hole keeping the charge diameter same, then we decrease the decoupling which means the shock wave does not lose its intensity, which it did when air was a medium between the rock and explosive. This subsequently increases the crushed zone around the borehole, inheriting a higher ratio of fine particles through that region. (Zhang X. , 2016) (Tete, 2013)

4.2.6 BURDEN/SPACING RATIO

The aspect of performing a sensitivity analysis was to provide a generic idea with reference to the aforementioned parameters. But an important aspect for every blast design is to determine an ideal burden/spacing ratio, depending upon the requirements.

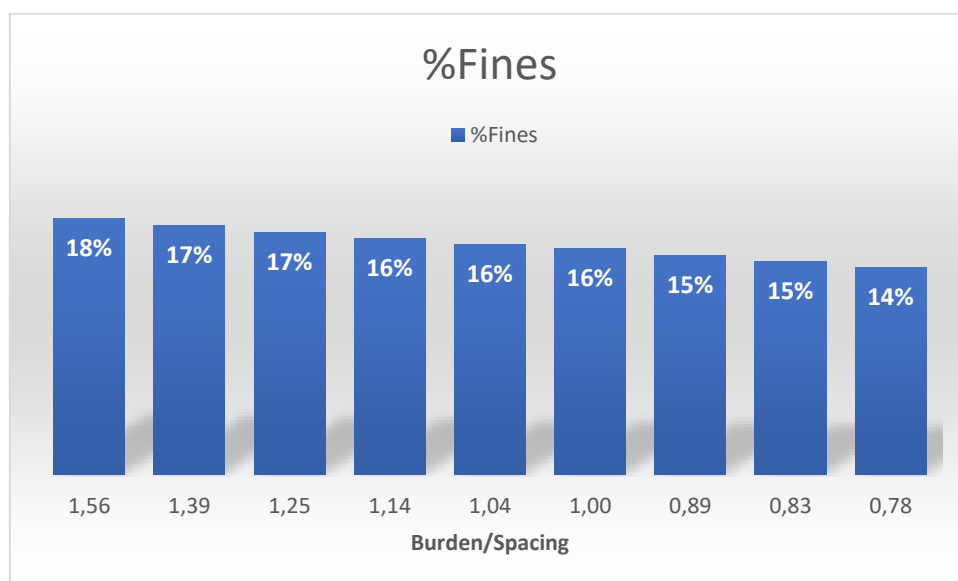


Figure 15 Burden-Spacing Ratio impact on Fine generation

Earlier we kept either of the parameters constant when the other was changed. Now after performing an analysis with changing both of them with respect to each other we find that it induces a drastic change in the outcome. Based on the Kuz-Ram model, if we increase the ratio we are finding ourselves with increasing fine particles in our fragmentation muck-pile. On the other hand, if we increase the spacing length more

than the burden then we decrease the fine generation. This can be understood easily if one understands the blast mechanism.

Increasing the spacing compared to burden length allows the shock wave to be generated in a drill hole that is unaffected by the shockwave generated from the neighbouring drill-hole. And since the burden is small as well therefore it will reach the free face sooner, losing most of its explosive energy and upon reflection from the free face with reduced energy the fragmentation would be resultantly coarser because the rock mass was not fractured adequately. (Sang, 2004)

4.2.7 SPECIFIC EXPLOSIVE ENERGY

This parameter is quite dependent upon the powder factor; therefore, the impact shall be the same on a global scale. As in, if the specific explosive energy is increased the fragmentation shall constitute a greater quantity of fine particles relatively to a blast that hold specific energy to be less. But an important aspect that needs to be considered here is the velocity upon detonation. (Kabwe, 2018) Though if the breakage is less than obviously powder factor would be low but the aspect of how it can be different for different scenarios even though the quantity of explosives is kept constant. This is observed with the fact that velocity upon detonation varies with the rock mass and the characteristics of the hole. If the hole is wet it is most common to have a coupling effect depending upon the type of explosive used and its tendency to detonation in wet conditions, that can be one aspect for its importance. Secondly, altering the quantity of each explosive in order to reduce the use of one explosive type can keep the total in a case to be same hence the powder factor but it can alter the fragmentation. Because if now the chosen explosive of the type with higher VOD is replaced with explosive of relatively lower VOD then that would mean that the SEE is less as well which will result in coarser fragmentation. (Tete, 2013)

4.2.8 BENCH HEIGHT

The aspect of changing bench height is not a straight forward decision since this induces other elements to be taken in regard, especially the equipment usage. If a 20-meter bench is divided into two benches of 10 m then a genuine feasibility study should be performed because with alteration like these it requires the practical aspect of checking whether the loading and hauling can be continued, or would it require adjustment to ramps and mine roadways.

Regardless of that still in the theoretical study part it was necessary to perform these changes, to understand the impact, further during the blast designing phase it would be argued with every key performance indicator in place for the changes.

To find the sensitivity of bench height, it is a common practice to analyse it with respect to the ratio to burden. The ratio is known as stiffness. We can argue for hypothetically for now that we keep the burden same and bring changes to the bench height. The results are showcased in the figure.

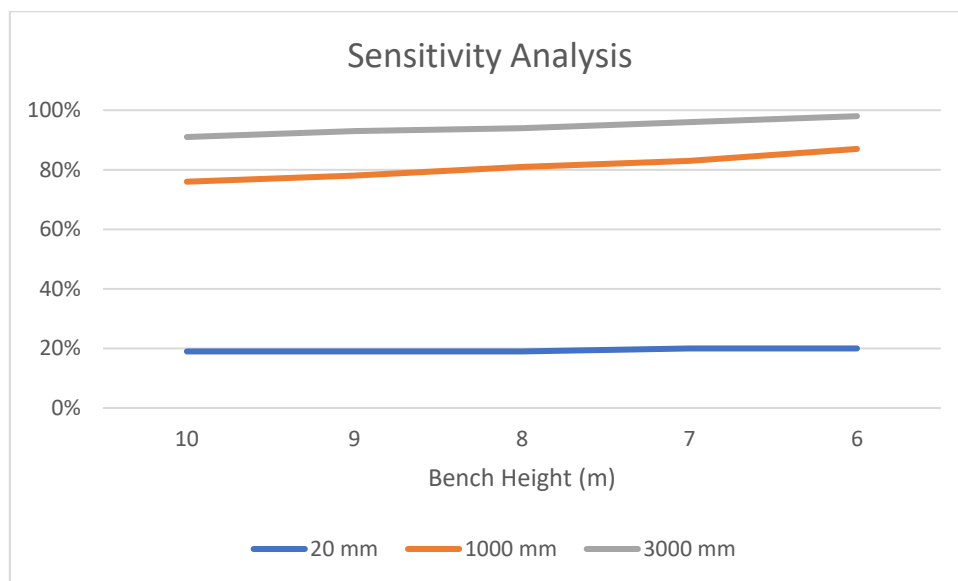


Figure 16 Impact of Bench Height over fragmented size

It can be seen, that change in bench height doesn't affect the generation of fine particles in fact the alteration impacts the coarser particle quantity. With decreasing bench height, since an increase is not possible for the current quarry scenario, the coarse particles passing a set sieve size increase. Observing the two line-segments of 1000mm and 3000 mm shows that, decreasing bench height reduces the Xmax as more particles are being generated in a set range. To explain this trend, see the figure.

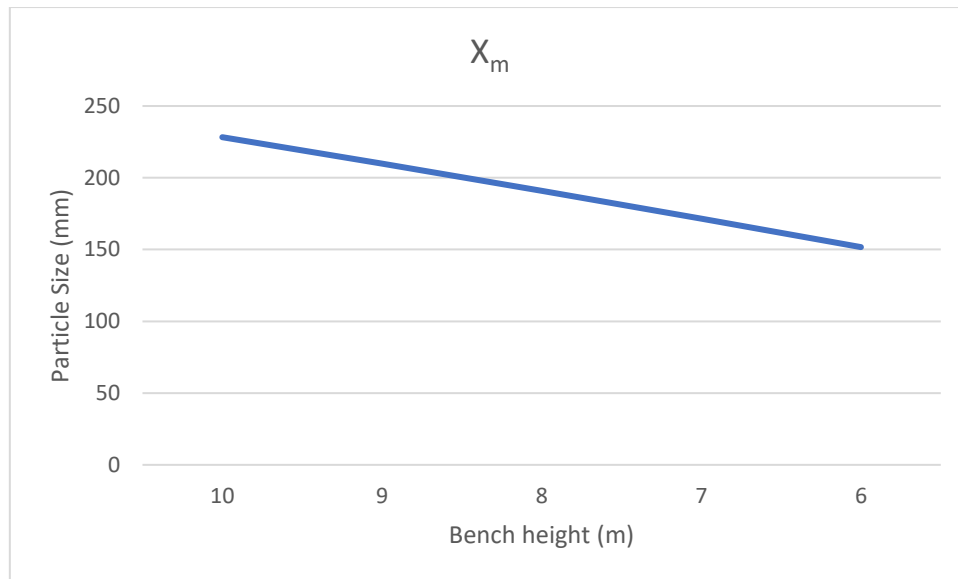


Figure 17 Bench height Impact on Particle Mean Size

The change in bench height causes the mean particle size to decrease with decrease in its value. If we consider our case in which we changed the bench height but kept the burden same, by decreasing the bench height we are decreasing the stiffness ratio, which implies, in terms of fragmentation, difficulty in displacing the rock, especially at the center (Ash R. , 1985). Smaller values for stiffness ratio can be understood as greater stiffness of the rock. Which in terms of material science is easily understandable as if the rock is bearing greater stiffness then it is resilient to breakage; most of the energy is absorbed by the rocks on its generation from the explosives, as rather than spreading across the zone of blast it is scatter down to the ground level as easily as it finds its way to the free face. This limitation confines the explosive energy in a small block. Therefore, it reduces the mean particle size but at the same time being lost in producing vibrations it does not produce as much fines as expected either. The absorption of energy on ground may cause fly rocks and cratering, apart from the vibrations. (Smith, 1976) (Singh, 2012)

5 MODEL VALIDATION

5.1 PURPOSE AND METHODOLOGY

To test the model for the quarry at Jemelle, prior implementation; it was necessary to perform a complete analysis of fragmentation for one test blast.

A blast was carried out on April 4, 2019. Prior to the blast the rock mass as shared in the methodology, was mapped to determine the Rock Mass Rating. Images of the bench were captured using a drone, DJI Mavic Pro 2. An additional platform, as assistance for drone, was used called DroneDeploy. The platform allowed the images to be stitched together forming an orthomosaic image. Secondly, it also performed the processing of acquiring a 3D image of the bench. The data from the platform is essential, as it can be used further in later studies as source for correlations. The bench was divided into zones, each zone comprised of 4-5 drill holes, hence for the case present each zone varied from 15-18 meters. The zones were then mapped for the discontinuities visible on the bench face. Based on the criteria presented in RMR system, the persistence, spacing, filling, RQD and Weathering was analysed for each zone separately. Using ImageJ, the discontinuities were distinguished. The results are showcased in the Figure 18. (Shang, 2018)

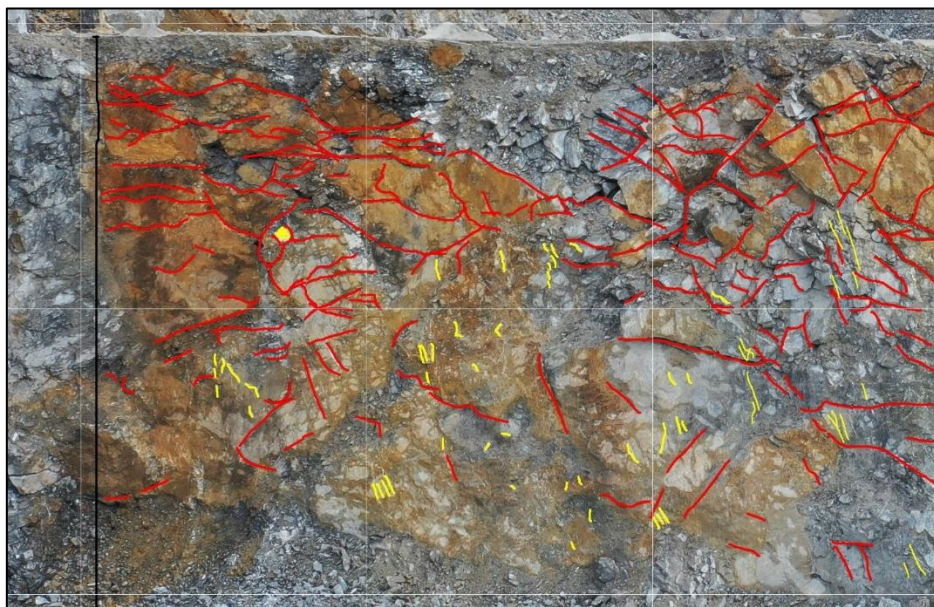


Figure 18 Discontinuities Sketching (Red: Discontinuity; Yellow: Filling), for scale use grid size 5m x 5m

Table 4 RMR Values for Each Zone in the Bench Face

ZONE	RMR
Z 1	68,43
Z 2	75,17
Z 3	71,80
Z 4	73,40
Bench Average	72,00

The rating system was followed as per the deductions from observation of each zonal face. The final rating was based upon average of the ratings deduced from the zone being divided in five subzones, the reason was to improve the estimation for the rock mass under study.

Once the zones were mapped, next step was to analyze the fragmentation. The blast fragmentation was imaged as well, using the drone and then the images were processed accordingly in 2D orthomosaic and 3D Object file. This orthomosaic and 3D file provided a real time viewing of the blast pile also, it gives physically safe viewing of the complete muck pile. Depending upon the number and quality of images captured, no details were missed and an in depth visual analysis was made possible.

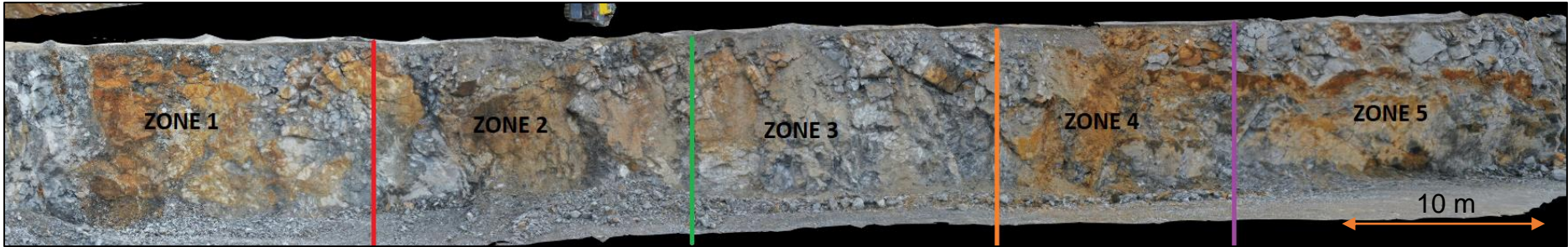


Figure 19 Face Zonal Division



Figure 20 Fragmentation Zonal Division

5.2 RESULTS AND DISCUSSION

Using WipFrag, the fragmentation was analysed, there was a certain difference in the results obtained from the software. Various methods were tried, the limitation and results for each of the analysis technique is shared to understand and provide information for usage of the software and possibilities with regard to its limitation.

Initially after blast the fragmentation was imaged by the drone at an altitude of 50 m, which gave the length of coverage to be 71 m. But due to the limitation of the software the images formed gave inconsistent results, because for the fines sorted in the fragmentation the pixel size was though 10mm per fine region but since the software has not yet upgraded itself to plotting the fraction of fines in the final PSD, obtained from a UAV image.

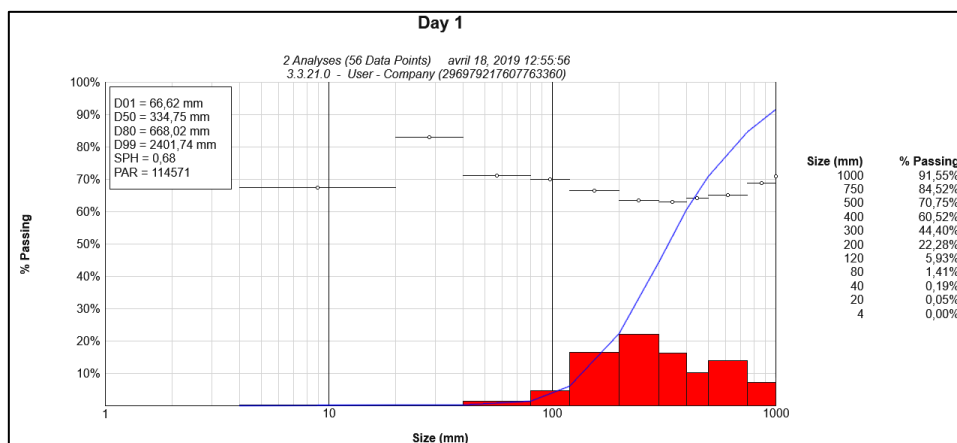


Figure 21 WipFrag Analysis for F2H Blast on April 4th, 2019

To counter this shortcoming of the software, another analysis was performed, this time the image was compressed and set as a regular image by opting for a non-UAV analysis. This is to mention that the images used were the same as earlier. The PSD acquired from the aforementioned analysis again gave an inconsistent result since now due to compression, detection of particles was difficult for the software and visually for user as well. Therefore, this decreased the number of particles detected and showcased the results. The results as well showed an anomaly based on the GSD for example in the day one statistic shown the smallest particle detected is 41 mm. which is not true, based on visual observation and measurements at site.

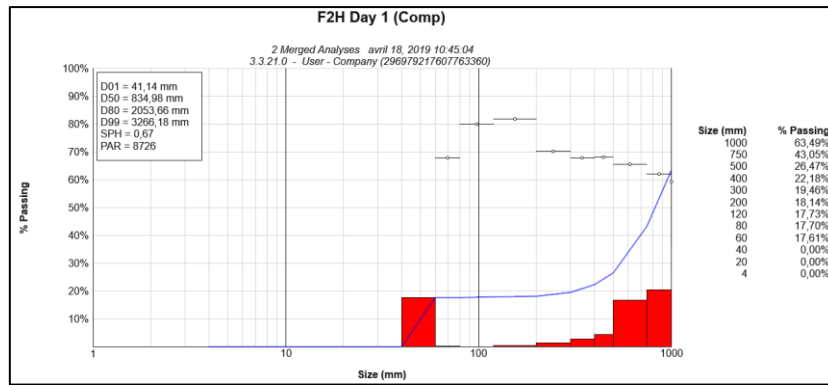


Figure 22 Wipfrag Analysis for Compressed Image of F2H Blast 4/4/19

A third method was implemented to understand and determine the fine particles. Since out of the two images the UAV image is with a higher resolution which consequently would be able to distinguish the coarse and fine particles compared to the compressed image. Therefore, in the image the fine region was outlined, and treated as one whole particle. The area of the particle was then calculated and followed up with summation of all such regions present in the pile. The sum was then compared with the total area of the pile. (See Appendix 11.8)

Table 5 Fine particles representation in the fragmentation pile for each day of imaging for F2H 4/4/19 Blast

DAY	TOTAL% FINES
1	7% - 8%
2	14%
3	21%

Since this method is inconclusive, due the idea that, focusing only the fines, without regarding the abnormality in calculation of rest of the particle size distribution, does not provide good outcome. Therefore, another method was proposed to reduce the region of analysis, this method would increase the tediousness in total processing time, as the number of images analysed for each blast shall increase but shall provide a possibility of another procedure for estimating accurate results. (G.C. Hunter, 1990) By accurate, the purpose is not to show the true distribution, which is not possible with 2D imaging, but to show a reliable size distribution. One that could showcase the variation in particles and shall not ignore any of the sized regions, or at least show the most promising result for data collection.

The current method, requires flying the drone at lower altitude than before, this lower height image consequently would have a reduced area of focus for each image, thus multiple images shall be processed for each muck-pile. In the current blast 9 images were processed, each image represented an average area of 345 m² of the muck pile. This method also requires imaging the pile at regular intervals so that changes in the profile of the muck-pile can be observed. As a note, the number of analyses processed for each muck-pile can be observed with the respective profile in the figure.

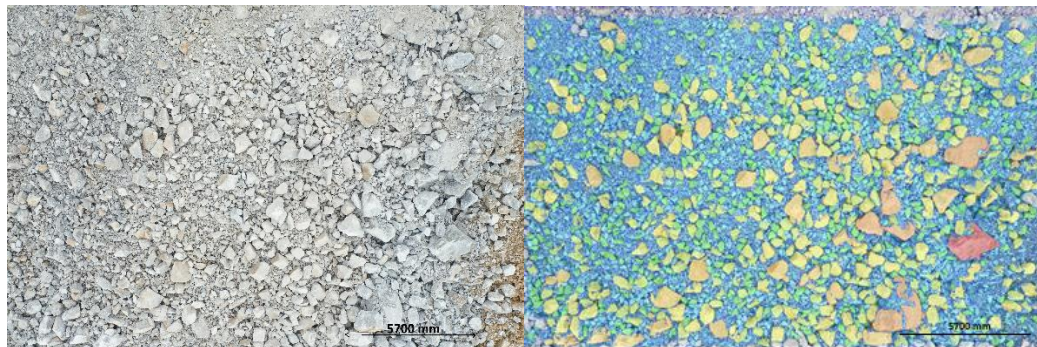


Figure 23 Analysis sample area from Blast 1, Left, original; Right, detected particles; color scheme denotes the size, red being largest and blue the smallest

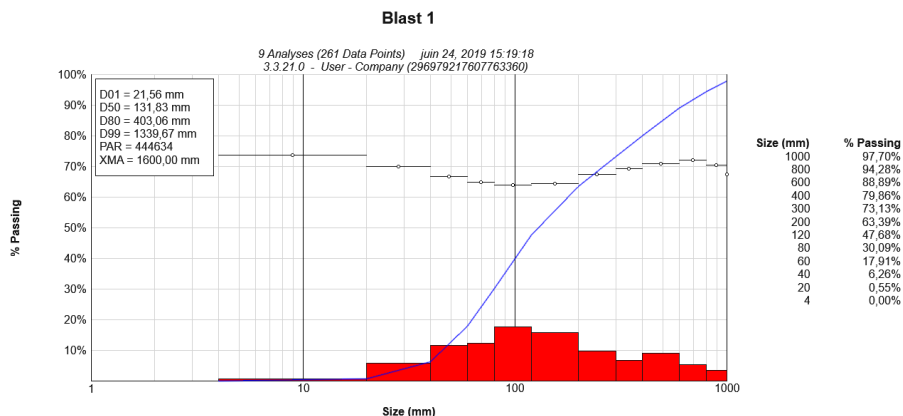


Figure 24 Wipfrag analysis following the reduced region exercise, result of 9 images merged together; F2H 5A, 4-4-19

The above curve from the blast, under study, was retrieved and furthermore correlated with the predictions from the Kuz-Ram model. The correlation was quite promising. Though, it can be observed that the particles under 100 mm are not well correlated as rest of the curve. But this again can be observed from the images, that it is difficult for the software to detect the respective sized particles with the chosen height. Therefore, all those detected are shown while for the rest it can be assumed, since the correlation is quite high, the rest of the curve can be assumed to follow the same trend. For these

curves, the area method for calculating the fine area was implemented but the region was not as large as experienced by images with large frame of references. Therefore, for effective and unbiased understanding, it was chosen to avoid that method and consider all the particles that the software and user can detect. Though in most cases the software detects the fine particles, as mentioned earlier, by merging them together as coarse particle but to counter that, in small regions, manually a mesh/grid is drawn that could represent these small size particles; if the region is too large and may cause extensive user rigor then that region is omitted out of the frame of reference for better estimation.

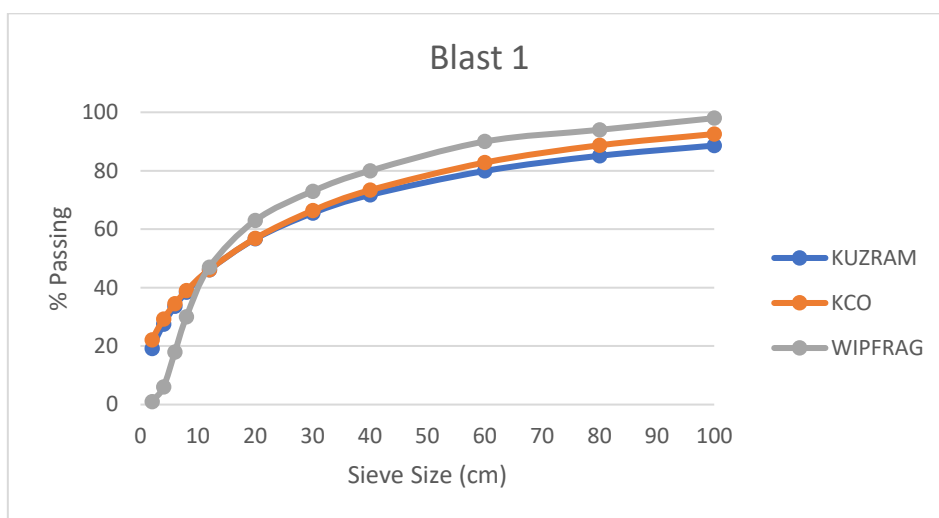


Figure 25 Comparison between empirical method and image analysis F2H 5A, 4-4-19

To further the assumption, it was practiced using the same method for a few more blasts in the period. (See Appendix 11.1) So, a new blast was chosen, and the method was followed. The Drone was flown at lower altitudes, over the fragmentation pile. Images were again followed up with analysis using WipFrag. As expected the size distribution was now broadened, though the distribution of particles below 20mm were still difficult to distinguish, which meant the drone was required to be flown at a lower altitude than practiced, but that would risk the safety of the equipment, since the sensory system may not comply well with the inhomogeneity in the pile height at different points. Therefore, it was avoided. (Maerz & Zhou, 2000)

The data reflected the similarity in the results as the correlation was sorted to be approximately the same, even with a different site, different rock mass. In fact, the lower altitude flight proved the theory that it was difficult to distinguish fine particles.

Since now the curve trends correlate well down to 60 mm. Hence, it was encouraged by these results, that the model could serve as basis for a new blast design.

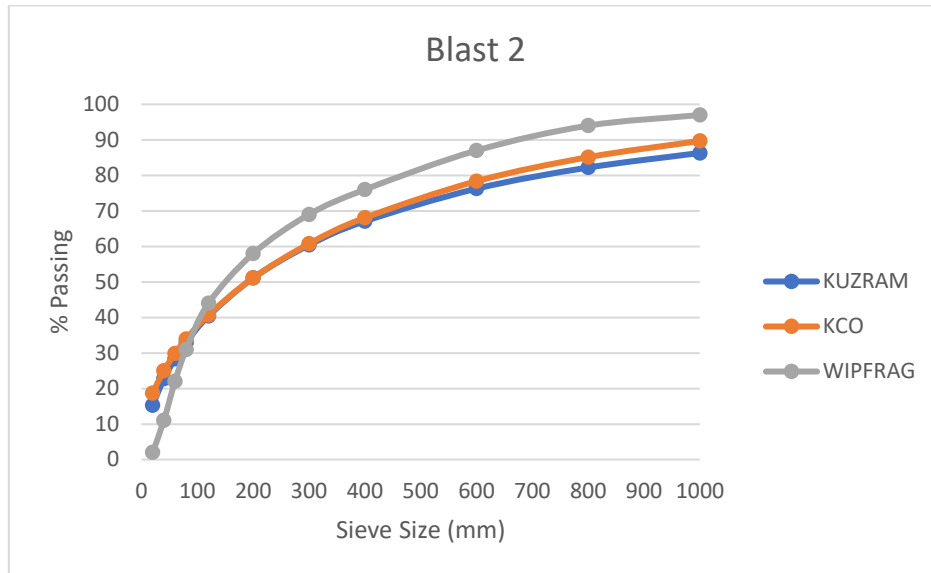


Figure 26 Comparison between the empirical methods and Image Analysis F2H 5B, 15-5-19

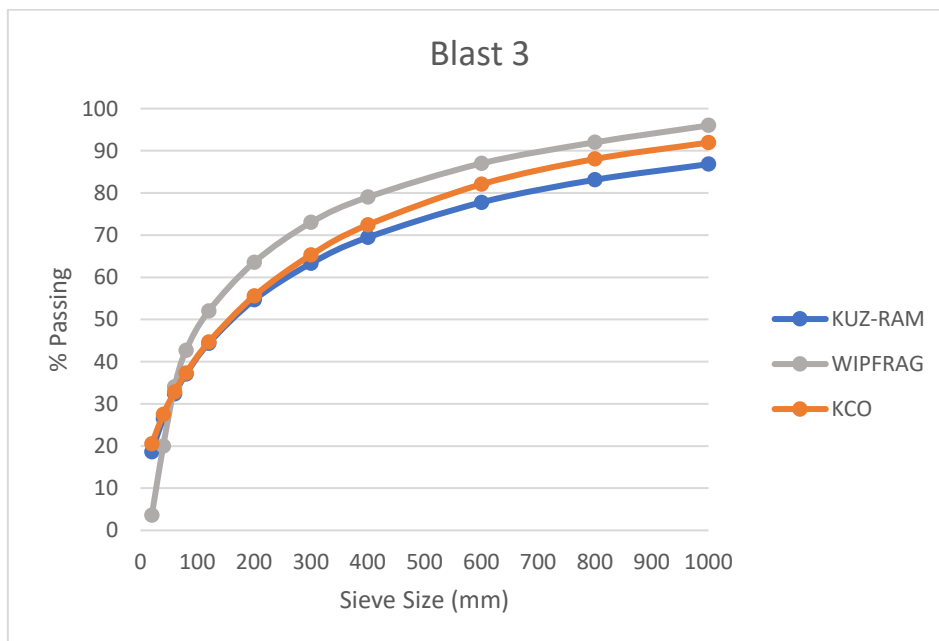


Figure 27 Comparison between empirical method and image analysis F2H 5A, 16-5-19

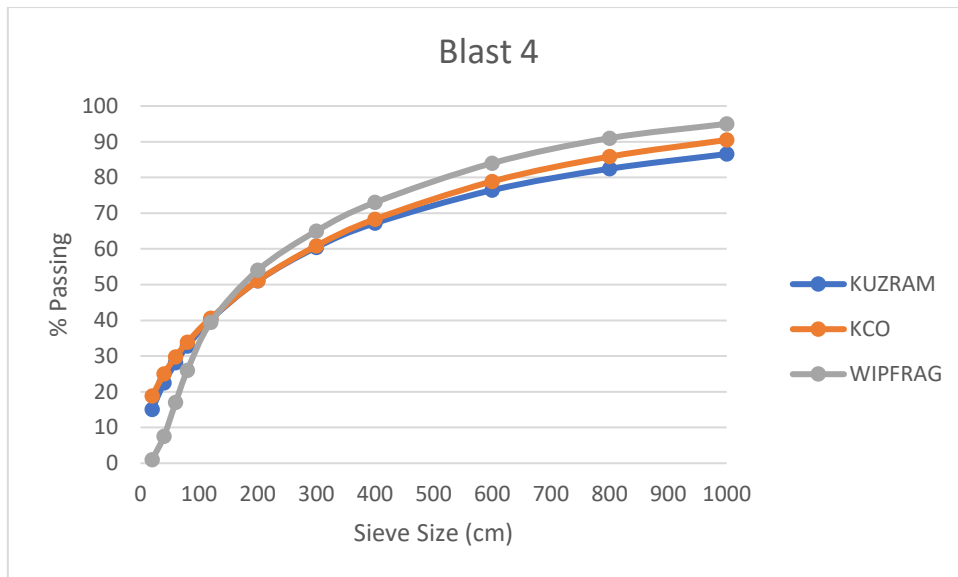


Figure 28 Comparison between empirical method and image analysis F2D 4, 23-5-19

5.2.1 CORRELATION AND RMS

A deduction was needed by performing correlation and calculating the Root mean square value for the output from the empirical methods and the image analysis. It can be seen that the correlation coefficient is very close to one, indicating a very strong correlation. For the RMS values the scores were not that large as well, in fact they showed a similarity between each other. Based on the results it was safe to say that Kuz-Ram applies well for the quarry under observation. (Barnston, 1992) (See Appendix 11.7). The first blast shows a stark difference than the rest for the reason that the images captured were from a higher altitude than the rest, which reduces the visibility and detection of smaller particles.

Table 6 Correlation and RMS values for Empirical and Image Analysis

Blast	Correlation Coefficient		RMS	
	Kuz-Ram	KCO	Kuz-Ram	KCO
1	0,99	0,983	11,39	11,52
2	0,995	0,993	9,65	9,77
3	0,982	0,987	8,25	8,22
4	0,997	0,992	8,82	9,38

5.2.2 BELT SCALE DATA TEST

Belt Scale system is installed at on the conveyor belts in the stone preparation plant to measure the feed tonnage conveyed on the belt for respective particle size. A test for correspondence of stone preparation plant, crushing factor and input from blast in 0/120 mm particle range was performed at the site, last year. That involved, feeding the crusher with a known feed tonnage and seeing the crushing factor and the weightage of each size range being produced, or already present in the feed. The data was retrieved and analysed with regard to the results acquired and predicted from the model. The data showed optimistic results for maintaining the trust in treating the Kuz-Ram Model as basis for new blast design.

Table 7 Belt Scale Data Test Results (Jemelle Plant, 2018)

Particle Size Range (mm)	Weighted % of Blast Fragmentation in mm	Cumulative %Passing with referenced Sieve Size
0/40	57,9%	23,22%
40/80	12,6%	28,22%
80/120	29,5%	40,07%

The test data showed that the final blast generates more than half of the total fine particles in production. The resulting figure of the 23,22% of 0/40mm passing through a Sieve of 40mm reflects the total percentage of fines that have directly been introduced by the blast. If we add the crushing input in generating fines, it sums up to 40,1%.

As mentioned this data showed quite similar trend and even close estimation with the prediction of the model. The entering values for this correlation required the average prediction from all the blasts. Since the feed for the test were an accumulated pile from either F2H and F2D, therefore to overcome that biasness average of the four blasts seemed to show better representation.

Table 8 Comparison of Model Results with Belt Scale Data Tests

Particle Size Range (mm)	Test Results	Kuz-Ram Model	Difference
0/40	23,22%	24,56%	+1,34
40/80	28,22%	35,23%	+7,01
80/120	40,07%	42,98%	+1,91

6 CORRELATION BETWEEN ROCK MASS AND FRAGMENTATION

6.1 PURPOSE AND METHODOLOGY

Since each of the bench holds a variation in the rock mass properties across its face; It was encouraged to see the impact of the rock mass over fragmentation and conclude an outcome from the experiment. (Akbari, 2015)

So, two regions were selected along the long bench of F2D on the 4th Level, varying in visual rock mass character. The selected zones were marked as Zone 1 and Zone 2.

To pursue on this task, the method shared earlier was followed. As in, mapping of the rock faces, tracing the visible discontinuities, testing the strength of the rock, analyzing the orientation and characteristics of the joints. This data shall aid in calculating the RMR for each Zone and furthermore help in devising a Rock Factor.

Since Rock Factor demands estimation of uniaxial compressive strength and Young's modulus, therefore, to estimate these values, empirical methods shall be performed, since practical examination requires arduous resources, for the lack there with, empirical method serve as a good alternative. Besides each of the calculated values shall be correlated with literature to see the estimation error.

Analysis after blast was necessary to see the difference between the fragmentation from the respective rock zone. Therefore, post-blasting, images were acquired and analysed with WipFrag. Comparison was made based on the model prediction and PSD based on the Image Analyses.

Furthermore, an exercise was followed in which these zones will be preferentially loaded to the crushing plant, utilizing the belt scale data, as if sieving was performed. This required coordinating with the loading and hauling staff and essentially needed marking the fragmentation, after blast was performed.

The loading proceeded in order, that first, the regions next to the zones were emptied, to provide safe access to these zones later and avoid rock falls and slips while loading. Then once these zones were marginally separated the task was followed. In which, each zone was designated a shift in which the loaded material would be fed to the plant. This would help in avoiding the contamination of data from each zone. Once the

feeding was finished for the shift the apron feeder was run till it was empty, yet again to avoid the stones from mixing and affecting our data collection. The loading cycle contributed 4170 t of stone to the plant, comprising both zones collectively (See table 8).

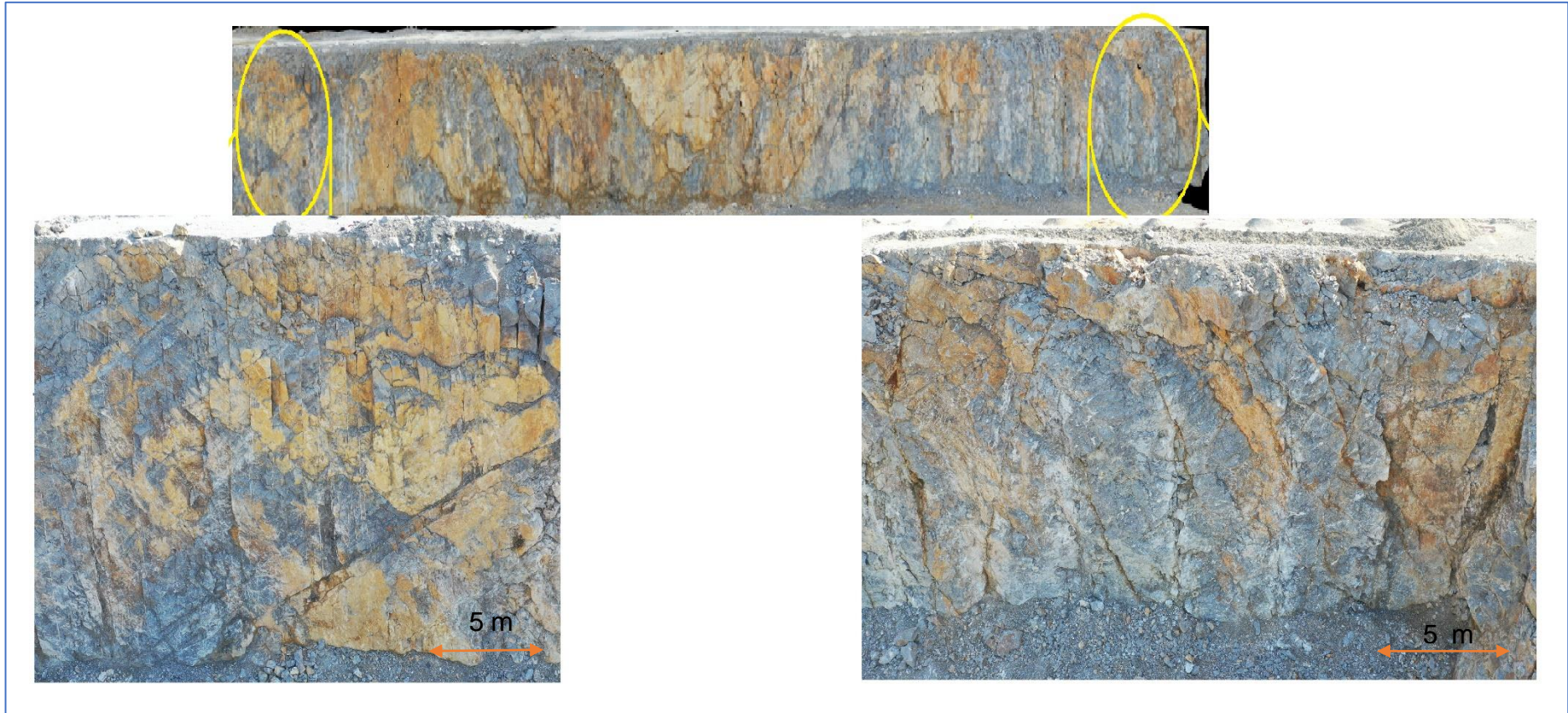


Figure 29 Zones from the bench; Right, Zone 1; Left, Zone 2

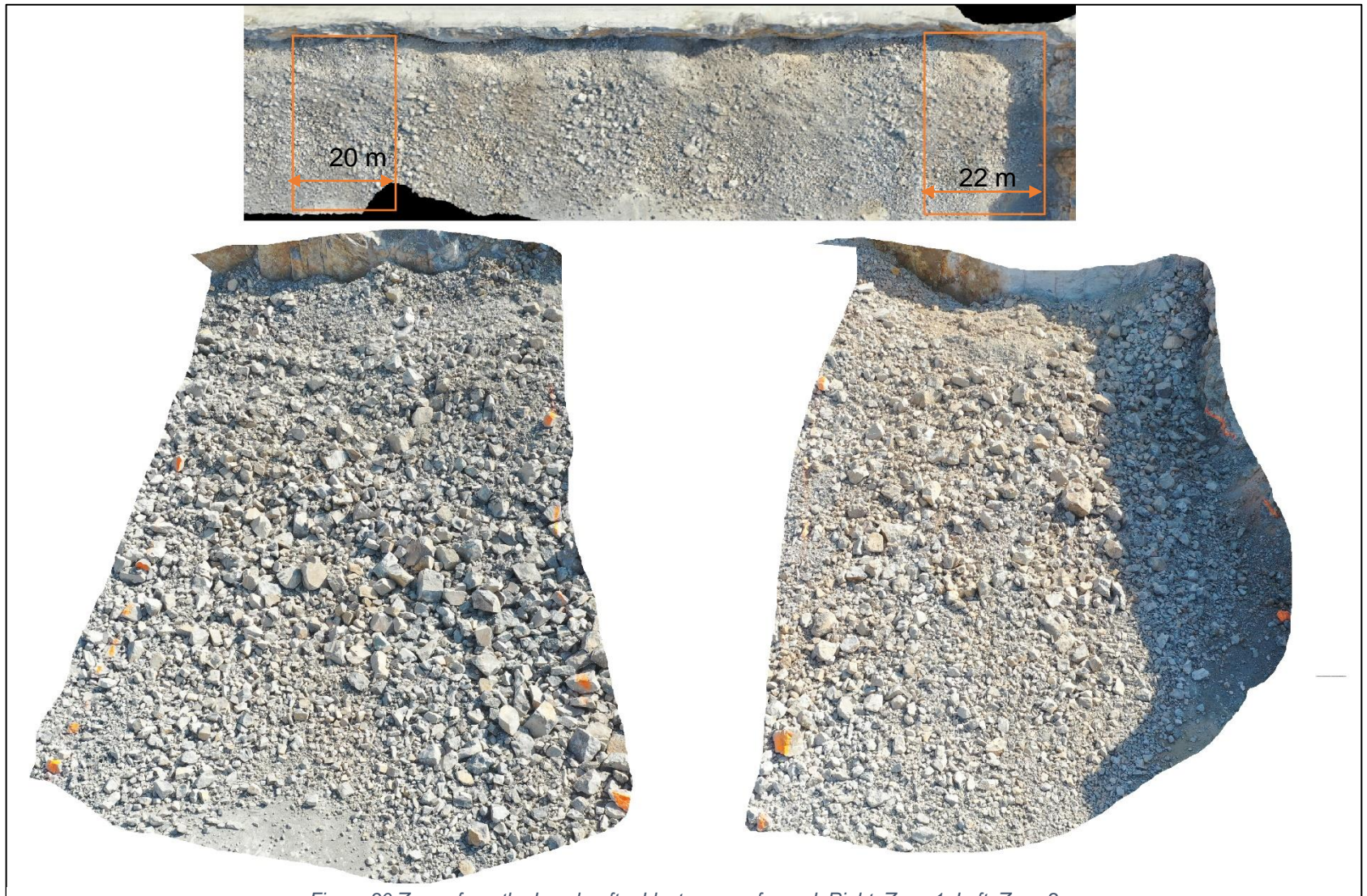


Figure 30 Zones from the bench, after blast was performed; Right, Zone 1; Left, Zone 2

6.2 RESULTS AND DISCUSSION

6.2.1 POINT LOAD STRENGTH TEST

The tests performed for each of the zones reverberated variable values for each of the sample collected from the zone. The reason for this variation can be based on the factor, that each of the rock sample has been affected one by the blast impact, secondly some of the rocks have sharp weakness zones that may be referred to as due to weathering or calcite filling, which provide fractures to occur along these locations. If a sample showcased fractures along these areas it was retested with the same block's daughter pieces. The result may sometime be starkly contrasting, yet, the fact that under the influence of blast, this can be the same reason for them to break. So, ignoring these values were not an option. Besides each of the zone being tested with multiple samples, the average of these values showed consistency in the value on a global average. Since the tests were performed for other benches as well for whom the model was validated, the similarity was observed in the values, showcasing that the strength of the rock altogether may not be the most impacting parameter, but still ignoring the statistic altogether is not advisable either. (See Appendix 11.3) (ASTM, 2016)

Nevertheless, the value from the point load strength was used to determine the UCS of the rock, which in return was used to determine the elastic modulus. (Ali et al, 2015)

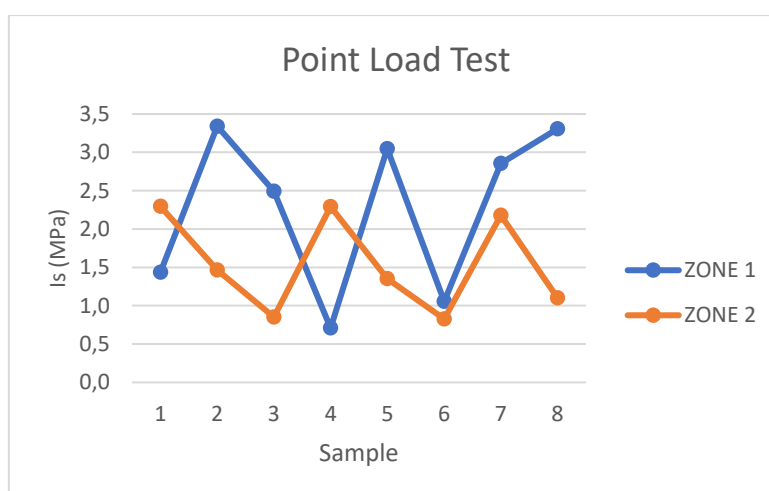


Figure 31 Point Load Testing Results for Each of the Two Zones

6.2.2 ROCK MASS RATING

The RMR values for the zones were determined using the same method. All the discontinuities were mapped with their necessary characteristics determined as required for the rating. This showcased a difference between each of the zones. Since some were more intact the rest. No relationship was deduced based on the geology of the rock mass in that area. As the test was based all on the images of face. The RMR value was introduced as a parameter along with the Point load strength value to determine the elastic modulus of the rocks from the zone. (Zhang L. , 2017)

It was noticed that both the zones presented a difference in their strength, Though the discontinuity features of Zone 2 seemed less influential therefore, the final rating turned out to be almost equivalent.

But since the study required that we only analyse the features evident over the face therefore deep insight into the rock mass was not possible and would affect the deductions based on theory.

6.2.3 ROCK FACTOR

Since Rock Factor is a determinant calculated from, the Rock Mass description, Hardness Factor and the Specific Gravity Influence. The measured value was made characteristic for each of the zone understudy. (Gheibe et al, 2009)

The discontinuity in the zone 1 were intersecting along each other, also It can be observed quite well that major plane of discontinuities is either dipping into face or out of face. While Zone 2 seems to show that most of the discontinuities planes were perpendicular to the face plane. This would impact explosive energy distribution across the rock mass. As it has been observed in cases where, discontinuities such as these give easy access for the gases to escape. (Konya et al, 1991)

Table 9 Comparison of Zonal Data Collected

		ZONE 1	ZONE 2
RMR		74,25	73,5
POINT LOAD STRENGTH		2,28 MPa	1,59 MPa
MAJOR JOINT ORIENTATION		DIPPING INTO AND OUT OF FACE	PERPENDICULAR DIPPING INTO FACE
ROCK FACTOR		4,04	4,24

6.2.4 FRAGMENTATION

Following the same suit as before, the parameters were all put as input for the model to predict the fragmentation in the designated zone. Followed up by the procedure to analyse fragmentation using image analysis for each zone to support the prediction of the model. This has to be kept in mind that even though the fragmentation is impacted by the quantity of explosives used in each drill hole, yet it has been assumed to be constant for each drill hole, consequently the zone, to see the impact for implication of the model at hand, besides the data for each drill hole is not available and the usual exercise is followed on intuition and experience by the blasting team. This may give biasness in the result but that shall be discussed accordingly, based on the data collected from site. Because on site nevertheless, the changes in explosive quantity is meager between each hole except if water is encountered in the borehole or drill hole was not drilled in an efficient manner, which may be due to maintaining the same drilling parameters for a rock zone that is stronger than the rest of the bench.

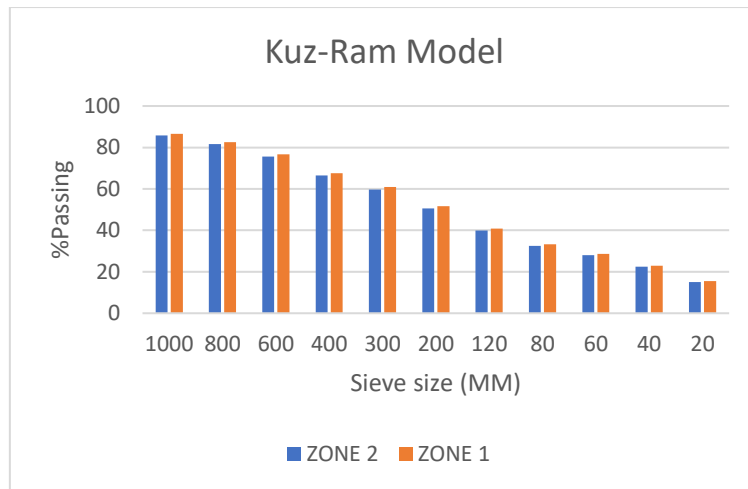


Figure 32 PSD prediction using Kuz-Ram Model

The difference in empirically predicted fragmentation is scarce for the reason that the model took the same value for almost each of the parameter except the Rock Factor, though it still gives off the idea that the Zone1 will give relatively finer fragmentation than Zone 2.

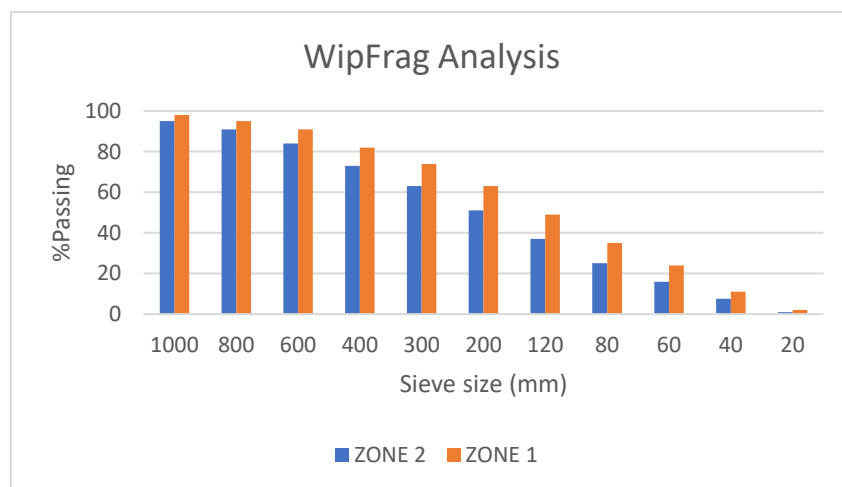


Figure 33 PSD for the Zones using Image Analysis

Image analysis of the fragmentation for each zone was performed and the result showed a difference in the particles under 120 mm. Which was predicted from the orientation of the visible joints, based on the assumption that the explosives quantity was the same in both regions the joints reduce the impact of explosives in breaking the rock effectively. Though another aspect was observed during the charging, that three of the drill holes in the zone 1 were water saturated. Which proves to be a better coupling medium than air, as the VOD and consequently the detonation pressure is

reduced in air by greater factor than in water. This could also be the reason why finer particles were relatively in higher excess in Zone 1 then in Zone 2; but at the same time in boreholes with water saturation, use of ANFO is avoided. (Konya et al, 1991) (Lyana, 2016) (Chakraborty, 1994)

As mentioned earlier these Zones were to be preferentially loaded in order to make use of the Belt scale system, in stone preparation plant, as sieving support. Though the system gives two broad regions for measurement, that is unhindered by the crushing unit, yet, it gives a good idea how the particle size distribution is followed in each of the zones.



Figure 34 Zonal view of the fragmentation after preferential loading cycles were followed.

Table 10 Belt Scale data from Stone Preparation Plant

Zone	0/120 (t)	0/120 %Total	120/1000 (t)	120/1000 %Total
Zone 1	770 t	44%	991 t	56%
Zone 2	939 t	39%	1470	61%

The data from the belt scale showcase a similarity to the prediction and also to the image analysis data. Though the variation in all is down to how each of the elements measure these numbers. Firstly, for the belt scale data, the number presented is an underestimation, since some of the particles are conveyed into the jaw crusher, bypassing the scalper, along with the coarse stones of above 120mm. The usual estimation is carried out to be 5-10% of the total feed of Jaw crusher. But calculating the exact quantity is far from possible with current tools.

Images analysed by Wipfrag are supposed to give a representative view of the complete fragmentation. Because as the rock mass is blasted the coarse rocks mostly end up on top of the pile, while the fines are in the center and bottom. During the analysis this limitation was somewhat overcome but not completely, by analyzing images after loading intervals, where new stones would be revealed.

As for the empirical model, well it has been formulated to give an idea, not the true results, and which fortunately in our case, yet again it did, by distinguishing the fact that Zone 2 shall give relatively higher coarse stones than Zone 1.

6.2.5 CONCLUSION

The exercise gave an idea of how fragmentation can respond to rock mass structure. The orientation of discontinuity is an important aspect that should be considered prior formulating the blast design. In order to achieve a homogeneity and desired fragmentation, each region of charging and blast designing should be adapted to its respective characteristics. Though the element of equivalent charge renders a question mark over the results, but the idea of charging only with emulsion still downplays that argument. Since emulsion charging is limited, and less emulsion in weight is used for each hole, for maintaining a certain charge length, compared to charging regularly with ANFO. Though, then the counter argument may arise that the Relative Weight Strength is greater with use of only emulsion but that is again limited in scope, since with using ANFO, it would reduce the impact of air medium by reducing the decoupling ratio, reducing the detonation velocity and consequently, pressure of the explosive shock wave. Another element which should have impacted the fragmentation for the zones was the strength of the rock, zone 2 showcased lesser strength therefore, it should have fragmented more but it was otherwise. To sum it up, though it may be quite difficult to state any fact without having the complete data but based on the current observations and limited collection of data it can be concluded that rock mass plays a major role in determining the muck-pile particle size distribution, which it did in the current scenario, by exhibiting a relatively coarser fragmentation for a zone with orientation of discontinuities that were favourable for explosive energy to escape and reduce its impact for fragmentation.

7 WAY FORWARD

Based on the data retrieved from the test and literature, there are certain proposals for alteration of blast design that can prove to be answers in optimizing the blast fragmentation particle size distribution. Which would mean that the new design shall reduce the number of fines (0/40mm) entering the primary crusher.

Since the Kuz-Ram model served as a good representation of the blast's fragmentation profile, therefore it would serve as a good starter for designing the future blast. Based on the theoretical outlook for changing some of major blast parameters, the model was tested for these various changes to somehow achieve a desired fragmentation profile. But this has to be kept in mind, how to proceed, as some parameters may be limited by skill level and equipment specifications. Therefore, great changes to model in first attempt shall not be proposed.

Therefore, to keep the aspect and be rational in using empirical model's data for practical measures it is proposed that we begin by changing the Spacing to Burden ratio. The current ratio is quite low, though keeping the burden same at this point shall be advised but increasing the spacing between the holes is what has been proposed. Because fragmentation, in theory, all is down to how blast mechanism works. If the hole spacing is small, there are possibilities for the two shock waves generated in neighbouring holes to coincide and break the rock further. Having a larger hole spacing may decrease this probability as the crushed zone for each hole may only be impacted by its own explosives. This alteration also proves to be the simplest in maneuvering for the drilling team, though it may be kept in mind that this will require a change in the quantity of explosives. Since this will increase the volume for each blast and maintaining the same powder factor, though in theory will, increase the coarse particle generation but to keep these alterations comprehensive in their impact it would be advisable to load the hole with approximately the same explosive quantity as previous blasts that have been performed. Because this will, as mentioned, showcase the impact of the fines generated in the crushed zone. Once that is proceeded. The data needs to be analysed, in reference to the data collected for previous blasts.

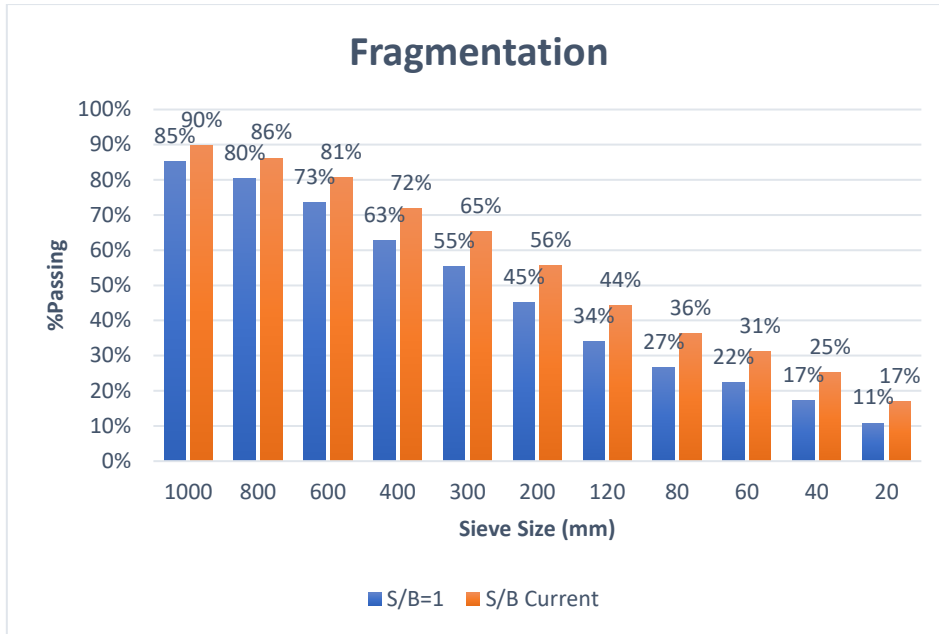


Figure 35 Difference in fragmentation with changed S/B ratio for F2H 5e bench, Blast of same bench on 16/5/19

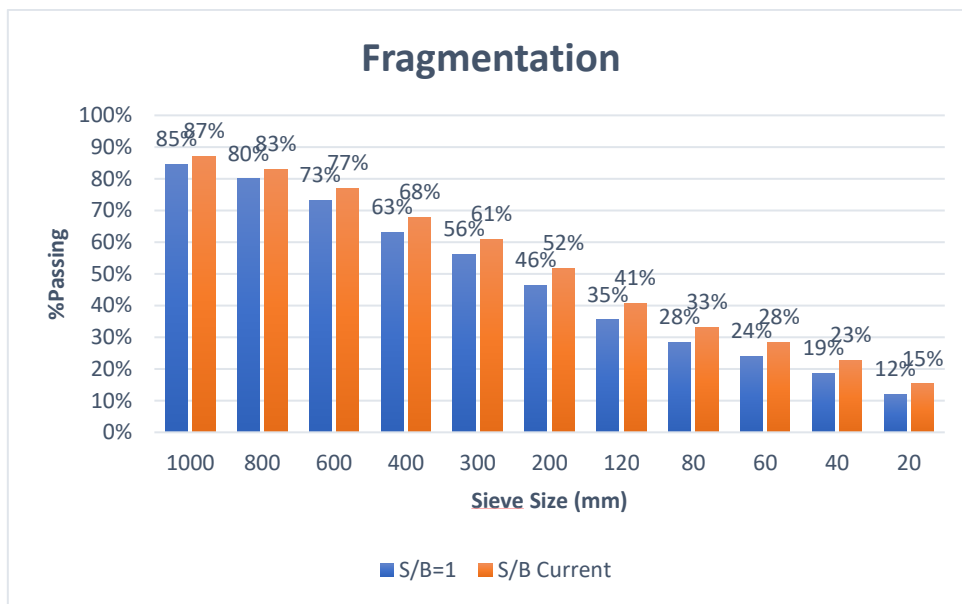


Figure 36 Difference in fragmentation with changed S/B ratio for F2D 4, Blast of same bench on 23/5/19

The figures show the difference achieved, if we follow up on the proposal for changing the spacing to burden ratio. Though one thing is quite evident that both the benches return a different PSD. Which though would be obvious in any case but in this case the reference is made to fact that the F2D bench already provides a better yield for the kiln, with reduced fine generation compared to F2H. The reason can be because the spacing to burden ratio in F2D is already higher than F2H. Though other elements do

come to play here as well, because the height of the F2D bench is greater than F2H, but then again, in theory that should not impact the generation of fines but can impact the average grain size. Secondly, the rock mass characteristic may differ but with our current zonal exercise we performed we saw the difference in general does not impact greatly, in theory, rather the orientation of discontinuity that may be influencing the fragmentation, in practice.

Therefore, to see this theory in practice we observe the results from the image analysis of the two blasts, we see the difference as well and that coincides well with the theory shared. For the blast of F2H, the values are taken as average for the two blasts that have been performed to compare, relatively closely to the quantity being blasted and the images being analyzed. (See Appendix 11.2)

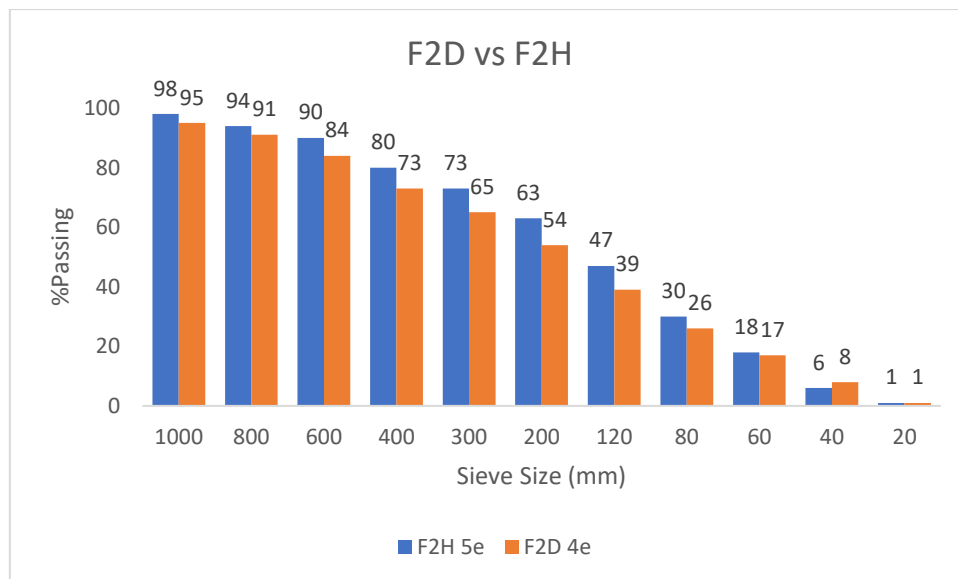


Figure 37 Image Analysis Result Comparison

Table 11 Parameters comparison between F2D 4e and F2H 5e

Parameter	F2D 4e	F2H 5e
Rock Factor	4,3	4,02
Powder Factor	0,44 kg/m ³	0,47 kg/m ³
Bench Height	14 m	9,5 m
Explosive/hole	171 kg	96 kg
Particle Mean Size (WipFrag)	179 mm	120 mm

We see from the histogram that F2D showcases less percentage of fines compared to F2H, even though the data of both the blasts seems to be the same, when it comes to powder factor and the explosive count. The theoretical higher mean particle size for higher stiffness ratio (Bench Height to Burden ratio) is observed in the analysis as well. Therefore, basing on these limited results, since we are not comparing the results of the particles detected under 80 mm, and the correlation we achieved with image analysis of the blast, that has already been performed, increasing the spacing to burden ratio could prove to be a way forward for optimization of the kiln feed yield.

Second step then would be then to test the influence of the explosive diameter, currently the diameter of explosives used is almost half of what the borehole diameter is, therefore most of the energy is wasted.(See Appendix 11.6) Though it must be said that it does decrease the energy responsible for fragmentation, which consequently would produce coarser particles but that can also be achieved by using explosives with lower strength.

Third step would refer to explosives as well with reference to its use in the model. Currently the model predictions are based on theoretical charge length which is certainly not correct. Because at the site, during charging, ANFO is poured in to the borehole as bulk explosive, which is assumed for the model as if it perfectly lines on top of the previously placed explosives, See figure 38. The current model estimation is in line because of this anomaly, when we assume a reduced charge length, it does not though affect the correlation with the image analysis result nor does it affect the region of particle size between 120-400 mm drastically, but it does affect the coarser region and the finer region above and beneath this region, respectively. Besides, we do not have the supporting materials of how exactly the ANFO is distributed down in the bore hole. Therefore, to keep it unbiased the matter is taken as optimum charge length, as mentioned earlier. This issue needs to be addressed on site as well, but to avoid this in the first-place, decking system can be installed right after the emulsions are placed, so now, the ANFO shall add up to the charge length from that point. Result of this blast then are needed to be correlated with the model and analysis to test the validity of the model. (Zhang , 2016). Nevertheless, decking shall add another element to the blast for consideration as well. Since, most of the the ANFO is filling up the

space between the packaged explosive, placed at the bottom, and the borehole, therefore it is affecting this region by producing excessive energy in the toe region and lower energy near the collar. This is why most of the faces after blasts had large boulders, that probably generated from the crest; additionally, it seems to be a continuous effect since for the next blast, crest already had huge cracks for boulders to be generated again, these fractures prove to be a source of explosive energy loss as well, thus, preventing from efficient usage of resources.

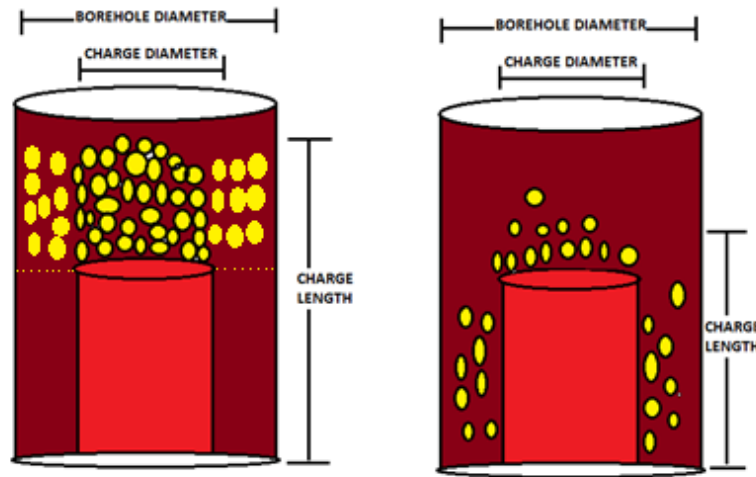


Figure 38 Difference in charge length between theoretical and actual; Left, Theoretical; Right, Actual (Schematic)



Figure 39 Example Image showing cracks post blasting in the crest region

To estimate the impact, of these minor changes, would require further tests and analysis of the blasts. The correlation can hold weigh only if there is continuous implementation of these theories. Because each blast is followed up by its impact over

the face and rock mass in total in the form of overbreaks or blast fractures. Therefore, the theory to consider individual parameters would lose ground in the scenario of basing it on one blast.

8 CONCLUSION

The study performed was to understand the different elements that could impact the fragmentation profile at La Boverie Quarry, Jemelle; and come about with reasons that could promote the attainment of Particle size distribution in accordance with the kiln feed requirement. The elements that were focused included the rock mass characteristics, the procedure of blast and the parameters undertaken in the blast design. Following conclusion were made, the conclusion also includes the learning from practices performed in achieving the aforementioned task;

- a) Using image analysis technique provides a good representation of fragmentation; that is possible only if the images are captured at lower altitude.
- b) Current WipFrag update does not support fine particle detection, empirical practices and estimations need to be performed for better outlook of the PSD. The software requires homogeneity in the lighting and imaging quality, which in outdoors cannot be maintained; therefore, extensive effort is needed for coverage of particles in each image.
- c) Using Drone's flight altitude can serve as a safer tool for scaling. Reduces the tendency of replacing the scale for each image. Also supports in considering the variability of muck-pile profile for estimating accurate scale sizes, though that was possible only with DroneDeploy platform, which serves as a good supportive tool for analyses and studies like this.
- d) Using empirical data and modelling can be used as a good starting tool for estimating and understanding blast designs.
- e) Current study projects, the data collected and analysed, correlates well with the prediction made with using Kuz-Ram Model.
- f) New design can be formulated using Kuz-Ram Model as basis.
- g) Rock mass characteristics play a major role in prospective particle size distribution of the muck-pile.
- h) Base on the current approach, Rock Mass Rating can not be called upon as a determinant for the blast, current exercises and data demanded such tests to have same blast design parameters, which were not maintained.
- i) Discontinuity and joints orientation should be thoroughly analysed for each blast.

- j) Spacing to burden ratio should be reexamined, as it suggests being a parameter that may infuse a reduction in fine particle generation, without requiring diligent effort in changing other parameters or skill level.
- k) Explosive diameter can serve to be an important element for analyzing blast mechanism; further study is needed to understand its impact, by decreasing the decoupling ratio.
- l) Decking system should be considered to avoid the spillage of ANFO down in the bottom; probably proving to be a source for fine generation in the toe region and boulders from the crest
- m) Data collection for each step is necessary for optimizing any operation.

9 RECOMMENDATIONS

Some recommendation shall be proposed in accordance to observations made during the period and the study performed

- a) The model does not take into account the detonation velocity of the explosive; therefore, impact of this property needs to be studied
- b) Cost analysis of each change being followed up in accordance with the model is required to be evaluated
- c) The impact of loading cycles should be performed with regard to changes in blast design, evaluation of this data can serve to improve cost efficiency in a longer run
- d) The current data considers four blasts, increasing the number of blasts for study shall improve the trust, consequently
- e) The study of rock mass involves user biasness, therefore follow up study with a team for reducing the factor is necessary for improved knowledge of the rock mass.
- f) Data collection for each blast performed is necessary; especially with explosives charging. Each hole should be treated as different than the other, therefore, data should be recorded for each hole, with reference to drill hole diameter, the amount and type of explosives used, the deviation in drilling.
- g) Probing of borehole properties may improve understanding the fragmentation as well. For future studies, if possible this should be adopted as one of the exercises.
- h) Currently the impact of water in borehole is subdued by using emulsions. But later tests can make use of decking, since placing emulsion does raise the level of water, so for knowledge of its impact, an alteration of such can be used, which in theory would reduce the generation of finer particles.
- i) Mechanical strength of the rock is weak; therefore, a comprehensive study needs to be performed in this regard to see its impact in fragmentation, upon loading and feeding.
- j) The current project is to increase the coarse particles by reducing the fines; A thorough study should be performed in optimizing the particle size that could maximize efficiency of the plant and process.

- k) One blast would never give a true picture because it will be impacted by the overbreak and underbreak of the previous blast. Therefore, each procedure should be followed more than once to insure true results.
- l) The scaling system followed with using the Drone altitude has been found to be approximately true, but to achieve precision it is advised to collect points using a GPS system and correlate with the readings.
- m) A study for analyzing kilns, installed at the plant, needs to be followed to understand the major reasons behind the lack of efficiency with the particle size fed.
- n) The model does not regard the detonator position, therefore proper analysis needs to be performed for optimizing the position for it.
- o) The belt scale data compiles all the feed from the quarry that is being loaded through the apron feeder. The system will rather optimize data collection if each bench is designated a certain time zone and is referenced in the data. This will provide a good estimation for fragmentation for each bench blast.

10 REFERENCES

- Akbari, M., Lashkaripour, G., Yarahamdi Bafghi, A., & Ghafoori, M. (2015). Blastability evaluation for rock mass fragmentation in Iran central iron ore mines. *International Journal of Mining Science and Technology*, 59-66.
- Ali, M., Mollali, M., & Yazdani, M. (2015). Correlation between uniaxial strength and point load index of rocks. *15th Asian Regional Conference on Soil Mechanics and Geotechnical Engineering (15ARC) 'New Innovations and Sustainability'*. Kyusho: Japanese Geotechnical Society.
- Anderson, T. (2010). Estimating particle size distributions based on machine vision. *Doctoral Dissertation*. Lulea University.
- Aruna D. Tete, D. A. (2013). Velocity of detonation (VOD) measurement techniques practical approach. *International Journal of Engineering and Technology*, 259-265.
- Ash, R. (1985). Flexural rupture as a rock breakage mechanism in blasting. *Fragmentation by blasting*, 24-29.
- Ash, R. L. (1968, January). The Design of Blasting Rounds. *Surface Mining*, 373-397.
- ASTM, A. S. (2016). Standard Test Method for Determination of the Point Load Strength Index of Rock and Application to Rock Strength Classifications. *ASTM D5731-16*. West Conshohocken, Pennsylvania, United States of America: ASTM International.
- Aswegen, H. V., & Cunningham, C. (1986). The estimation of fragmentation in blast muckpiles by means of standard photographs. *South African Institute of Minerals and Metallurgy*, 469-474.
- Barnston, A. G. (1992). Correspondence among the Correlation, RMSE and Heidke Forecast Verification Measures; Refinement of the Heidke Score. *Notes and Correspondence*, 699-709.
- Bieniawski, Z. (1976). Rock mass classification in rock engineering. *Exploration for rock engineering, proc. of the symposium* (pp. 97-106). Cape Town: Balkema.
- Bonneville, P. (1980). A Study of Size Distribution by Photography Analysis. Queen's University.

- Borg, R. C. (1983). Increasing productivity through field control and high-speed photography. *Proc., 1st Int. Symp. on Rock Fragmentation by Blasting*, (pp. 301-331). Lulea.
- Chakraborty, A., Jethwa, J., & Paithankar, A. (1994). Assessing the effects of joint orientation and rock mass quality on fragmentation and overbreak in tunnel blasting. *Tunnelling and Underground Space Technology*, 471-482.
- Choudhary, B. S., & Sonu, K. (2013, December). Assessment of powder factor in surface bench blasting using schmidt rebound number of rock mass. *International Journal of Research in Engineering and Technology*, 02(12), 132-138.
- Coen-Aubert, M., & Boulvain, F. (2006). Frasnian. *Geologica Belgica*, 19-25.
- Cooper, P. (1996). Acceleration, formation and flight of fragments. In P. Cooper, *Explosives Engineering* (pp. 385-394). Wiley-VCH.
- Cunningham, C. (1983). The Kuz–Ram model for prediction of fragmentation from blasting. *Proceedings of 1st International Symposium on Rock Fragmentation by Blasting*, (pp. 439-454). Lulea.
- Cunningham, C. (2005). The Kuz-Ram Model-20 years on. *Brighton Conference Proceedings*, (pp. 201-210).
- E. Lopez Jimeno, C. J. (1995). *Drilling and Blasting of Rocks*. CRC Press.
- Fragblast 9. (2009). Rock Fragmentation by Blasting. In J. Sanchidrian (Ed.), *Proceedings of the 9th International Symposium on Rock Fragmentation By Blasting - FRAGBLAST 9* (p. 853). Grenada: CRC Press/Balkema.
- Francisco Leite, V. M. (2018). Pattern Expansion Optimization Model based on fragmentation analysis with Drone Technology. *Fragblast 12: 12th international Symposium on Rock Fragmentation by Blasting*. Lulea.
- Frédéric Boulvain, B. D., & Coen-Aubert, M. (2005). Frasnian Carbonate Buildups Of Southern Belgium: The Arche And Lion Members Interpreted As Atolls. *Geologica Belgica* , 69-89.
- G.C. Hunter, C. M. (1990). A review of image analysis techniques for measuring blast fragmentation. *Mining Science and Technology*, 11(1), 19-36.

- Ghose, A. (1988). Design of drilling and blasting subsystems—a rock mass classification approach. *Proc. Mine Planning and Equipment Selection*, 335-340.
- Gregory M. Dering, S. M. (2019). Review of drones, photogrammetry and emerging sensor technology for the study of dykes: best practises and future potential. *Journal of Volcanology and Geothermal Research*, 148-166.
- Gustafsson, R. (1973). *Swedish Blasting Technique*. Gothenberg: SPI.
- Hagan, T. (1992). Safe and cost-efficient drilling and blasting for tunnels, caverns, shafts and raises in India. *Proc. of a Workshop on Blasting Technology for Civil Engineering Projects*, (pp. 7.4-7.5). New Delhi.
- Hustrulid, W. (1999). *Blasting Principles for Open Pit Mining*. Rotterdam: A.A Balkema.
- J.Shang, L. W. (2018). Geological discontinuity persistence: Implications and quantification. *Engineering Geology*, 41-54.
- Jethro Michael Adebola, O. D. (2016). Rock Fragmentation Prediction using Kuz-Ram Model. *Journal of Environment and Earth Science*, 110-115.
- John Rusnak, C. M. (1997). *Using the Point Load Test to Determine the Uniaxial Compressive Strength of Coal Measure Rock*. Retrieved May 20, 2019, from CDC - The National Institute for Occupational Safety and Health (NIOSH): <https://www.cdc.gov/niosh/mining/UserFiles/works/pdfs/utplt.pdf>
- Kabwe, E. (2018). Velocity of detonation measurement and fragmentation analysis to evaluate blasting efficacy. *Journal of Rock Mechanics and Geotechnical Engineering*, 10(3), 523-533.
- Kecojevic, V., & Komljenovic, D. (2007, January). *Impact of Burden and Spacing on Fragment Size Distribution and Total Cost*. Retrieved May 4, 2019, from ResearchGate: https://www.researchgate.net/publication/261061905_Impact_of_Burden_and_Spacing_on_Fragment_Size_Distribution_and_Total_Cost_in_Quarry_Mining/
- Konya, C. J., & Walker, E. J. (1990). *Surface Blast Design*.
- Konya, C. J., & Walter, E. J. (1991). *Rock Blasting and Overbreak Control*. Mclean, Virginia: US Department of Transportation.

- Liu Changyou, Y. J. (2017, September). Rock-breaking mechanism and experimental analysis of confined blasting of borehole surrounding rock. *International Journal of Mining Science and Technology*, 27(5), 795-801.
- Lyana, K., Z.Hareyani, Shah, A., & Hazizan, M. (2016). Effect of Geological Condition on Degree of Fragmentation in a Simpang Pulai Marble Quarry. *Procedia Chemistry*, 694-701.
- Maerz, N. (1999). Online fragmentation analysis: Achievements in the mining Industry. *Center For Aggregates Research (ICAR) 7th Annual Symposium TX*.
- Maerz, N. H., & Zhou, W. (2000). Calibration of Optical Digital Fragmentation Measuring Systems . "Fragblast, *The International Journal For Blasting and Fragmentation*, 126-138.
- Maerz, T. C. (1999). Case Studies using the WipFrag Image Analysis System. *FRAGBLAST 6, Sixth International Symposium For Rock Fragmentation By Blasting*, (pp. 117-120). Johannesburg.
- Norbert H. Maerz, T. C. (1996). WipFrag Image Based Granulometry System. *Proceedings of the FRAGBLAST 5 Workshop on Measurement of Blast Fragmentation*, (pp. 91-99). Montreal.
- Oates, J. A. (1998). Lime and limestone: chemistry and technology, production and uses. Wiley-VCH .
- P.K. Singh, M. R. (2016). Rock fragmentation control in opencast blasting. *Journal of Rock Mechanics and Geotechnical Engineering*, 225-237.
- Paul Singh, R. N. (2007). The Influence of Rock Mass Quality in Controlled Blasting. *26th International Conference on Ground Control in Mining*.
- Porter, C. N. (1974). A comparison of theoretical explosive energy and energy measured underwater with measured rock fragmentation. *Proc. 3rd ISRM Congress*, (pp. 1371-1375).
- Rai, P., & Yang, H.-S. (2010). Investigation of Some Blast Design and Evaluation Parameters for Fragmentation in Limestone Quarries. *Tunnel and Underground Space*, 183-193.

- S.Gheibe, H.Aghababa, & S.H.Hoseini, Y. (2009). Modified Kuz—Ram fragmentation model and its use at the Sungun Copper Mine. *International Journal of Rock Mechanics and Mining Sciences*, 963-973.
- S.P. Singh & H. Abdul. (2012). Investigation of blast design parameters to optimize fragmentation. *Proceedings of the 10th Int.Symp. on Rock Fragmentation by Blast*, (pp. 181-185).
- Sang, H. C., & Katsuhiko, K. (2004). Rock Fragmentation Control in Blasting. *Materials Transactions*, 1722-1730.
- Sauvage, A. (2012). Applied method integrating rock mass in blast design. In P. Singh, & A. Sinha, *Rock Fragmentation by Blasting - Fragblast 10* (p. 872). London: CRC Press.
- Smith, N. (1976). Burden Rock Stiffness and Its Effect on Fragmentation in Bench Blasting. *PHD Thesis*. Rolla: University of Missouri.
- Souza, J. C., Silva, A. C., & Rocha, S. S. (2018, March 1). *Tmm Article: Analysis Of Blasting Rocks Prediction And Rock Fragmentation Results Using Split-Desktop Software*. Retrieved May 20, 2019, from *Technologia em Metallurgia, Materials e Mineração*: <http://www.tecnologiammm.com.br/doi/10.4322/2176-1523.1234>
- Thomas Bamford, K. E. (2017, August 21). *Aerial Rock Fragmentation Analysis in Low-Light Condition Using UAV Technology*. Retrieved from *arxiv.org*: <https://arxiv.org/abs/1708.06343>
- Thurley, M. (2002). Three dimensional data analysis for the separation and sizing of laboratory. *Doctoral Dissertation*. Clayton: Monash University.
- Thurley, M. (2011). Automated online measurement of limestone particle size distributions using 3D range data. *Journal of Process Control*, 254-262.
- Tim Chuen Pong, R. M.-H.-Z. (1983, December). The application of image analysis technique to mineral processing. *Pattern Recognition Letters* 2, 117-123.
- Vedala, R. S. (1987). An Investigation into the effect of blast geometry on rock fragmentation. *6th ISRM Congress*. Montreal: International Society for Rock Mechanics and Rock Engineering.

Zhang, L. (2017). Evaluation of rock mass deformability using empirical methods - A review. *Underground Space 2*, 1-15.

Zhang, X. (2016). *Rock Fracture and Blasting*. Oxford: Butterworth-Heinemann.

11 APPENDIX

11.1 BLAST PARAMETERS

Table 12 Blast Parameters for the four blasts analyzed

Parameter	Blast (4/4/19)	1 Blast (15/5/19)	2 Blast (16/5/19)	3 Blast (23/5/19)	4
Burden (B)	6 m	6 m	6 m	6 m	
Spacing (S)	3,5 m	4 m	3,5 m	4,5 m	
Rock Factor (A)	3,99	4,42	4,1	4,33	
Relative Weight Strength (RWS)	108,0947	110,75	111,3125	107,0828	
Powder Factor (K)	0,492 kg/m ³	0,402 kg/m ³	0,453 kg/m ³	0,438 kg/m ³	
Mass of Explosive (Q)	97,93 kg/hole	111,11 kg/hole	95,23 kg/hole	171,59 kg/hole	
Hole Diameter (h)	140 mm	140 mm	140 mm	140 mm	
Bench Height (H)	9,5 m	11	9,5 m	14 m	
Sub-Drilling	0,5 m	0,5 m	0,5 m	0,5 m	
Drill-holes	23	27	21	44	
Density of Rock	2,6 kg/m ³	2,6 kg/m ³	2,6 kg/m ³	2,6 kg/m ³	

11.2 WIPFRAG ANALYSIS

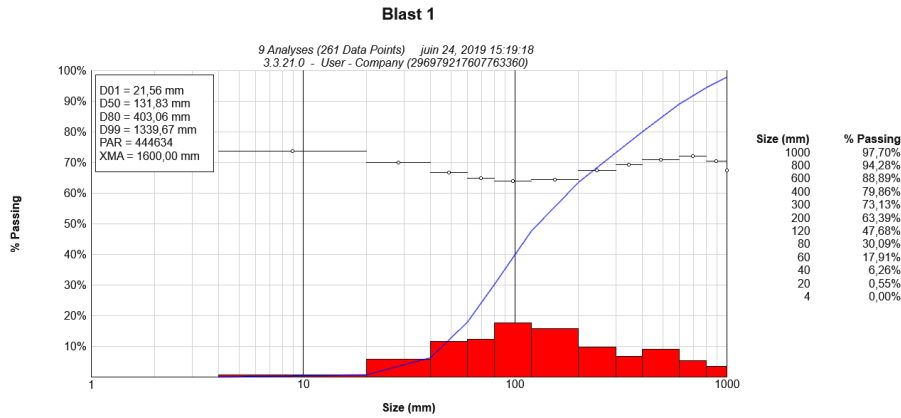


Figure 40 WipFrag Analysis for Blast 1, 9 images merged together; F2H 5A, 4/4/19

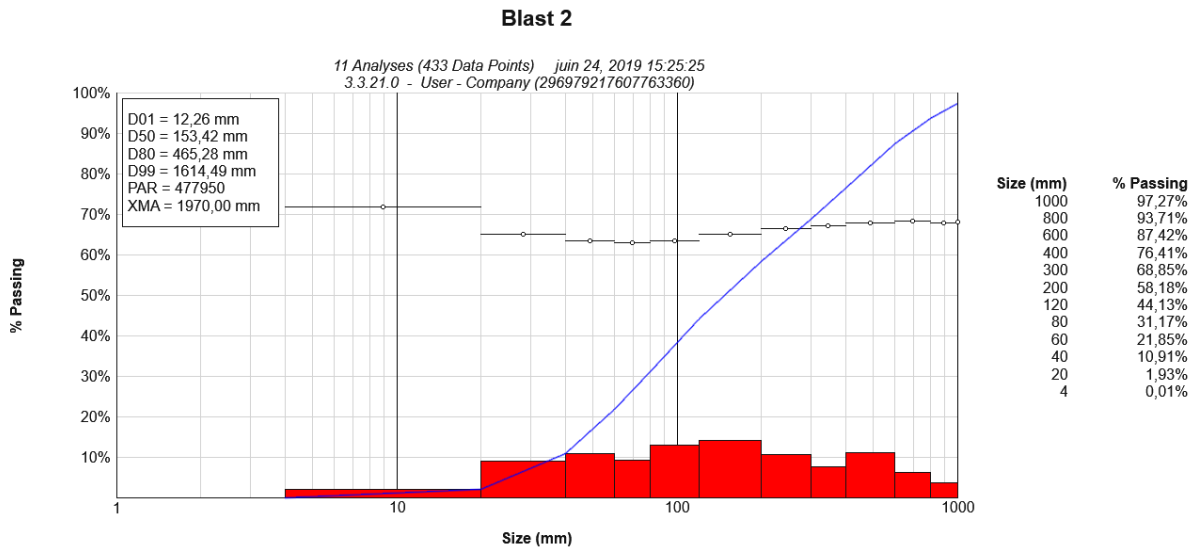


Figure 41 WipFrag Analysis for Blast 2, result from 11 merged images; F2H 5B, 15/5/19

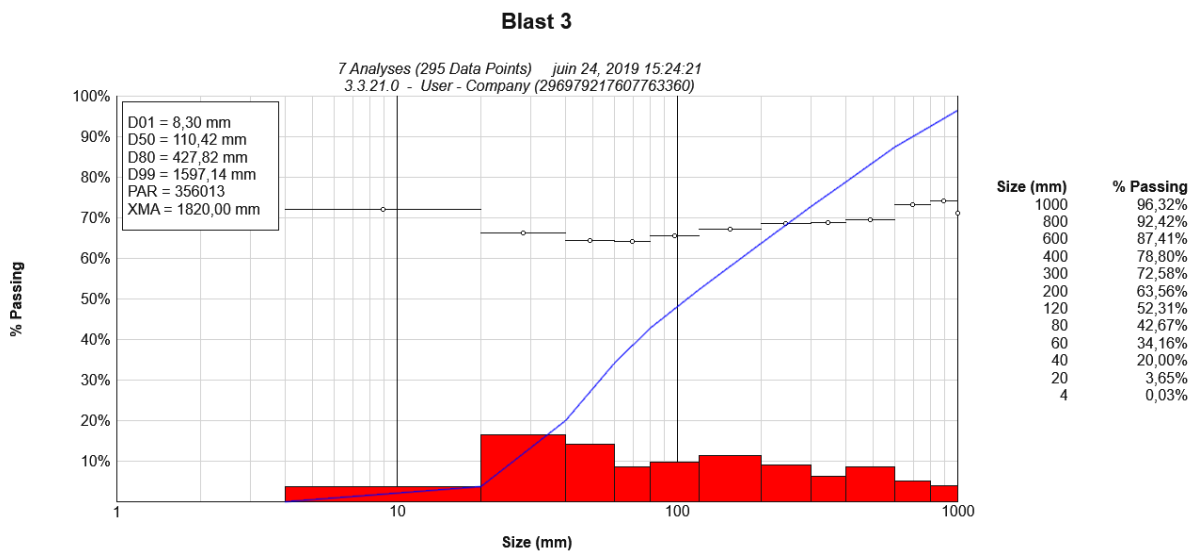


Figure 42 WipFrag Analysis for Blast 3, result from 7 merged images; F2H 5A, 16/5/19

Blast 4

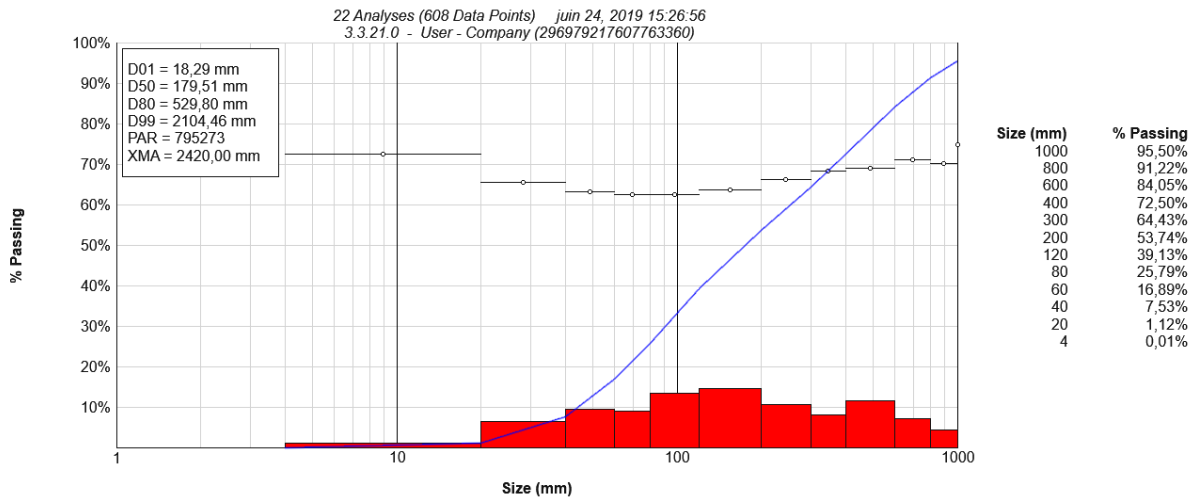


Figure 43 WipFrag Analysis for Blast 4, result from 22 merged images; F2D 4, 23/5/19

ZONE 1 F2D

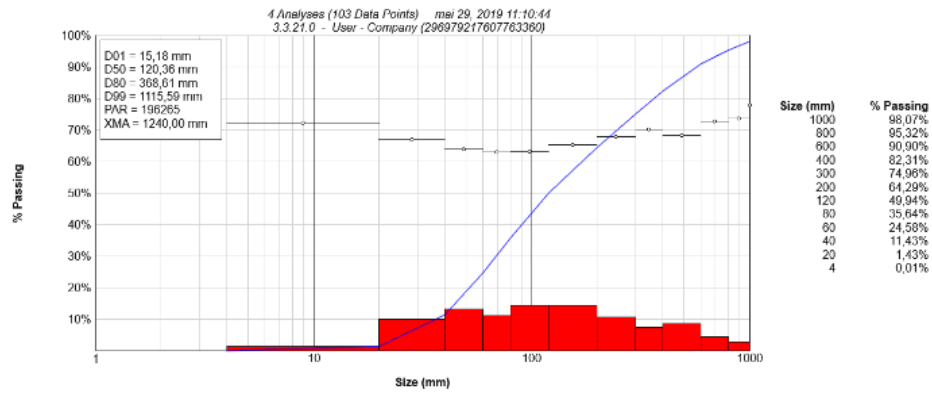


Figure 44 WipFrag Analysis for Zonal Exercise, result from 4 merged images; Zone 1, F2D 4, 23/5/19

ZONE 2 F2D

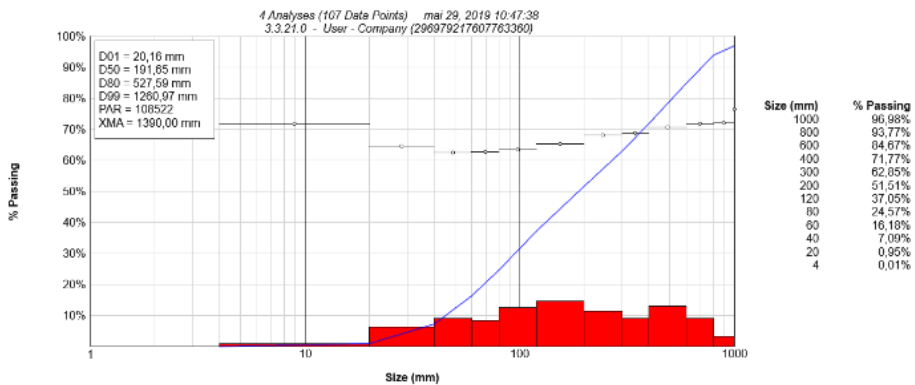


Figure 45 WipFrag Analysis for Zonal Exercise, result from 4 merged images; Zone 2, F2D 4, 23/5/19

11.3 POINT LOAD TEST



Figure 46 Example of Samples for Point Load Test Prior test and post-testing

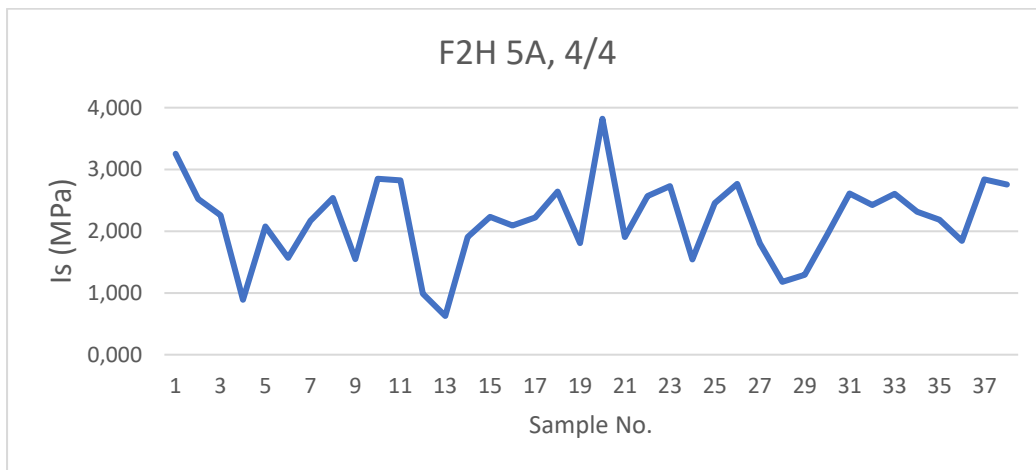


Figure 47 Point load strength for Blast 1 bench

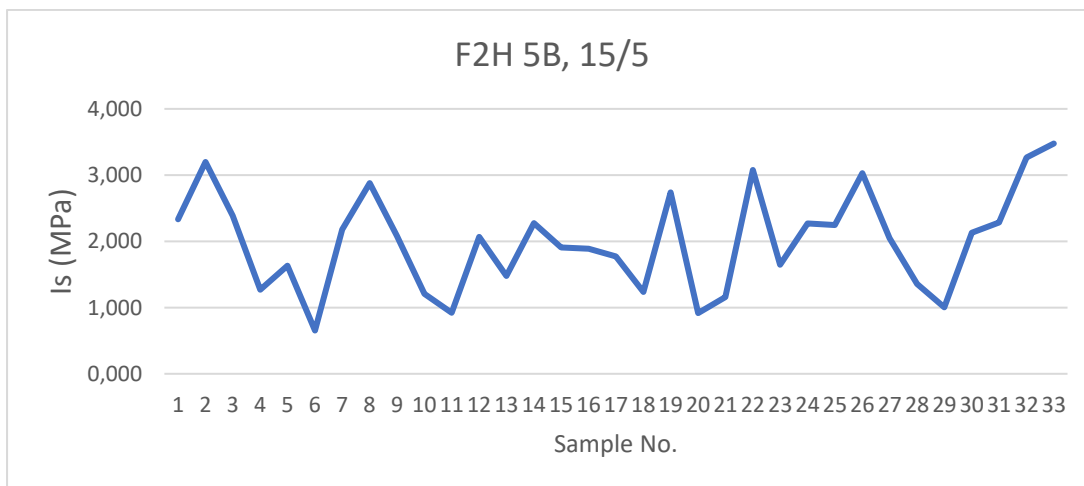


Figure 48 Point Load Strength for Blast 2 bench

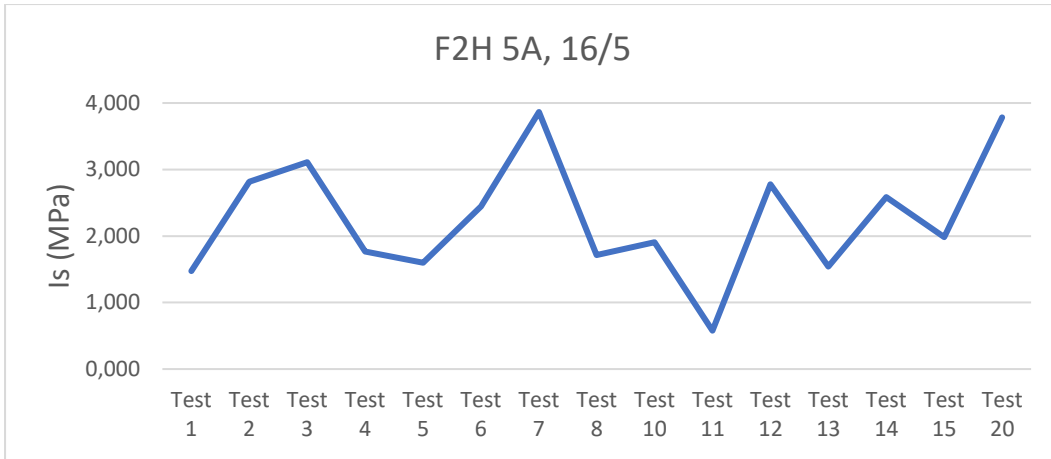


Figure 49 Point Load test for Blast 3 bench

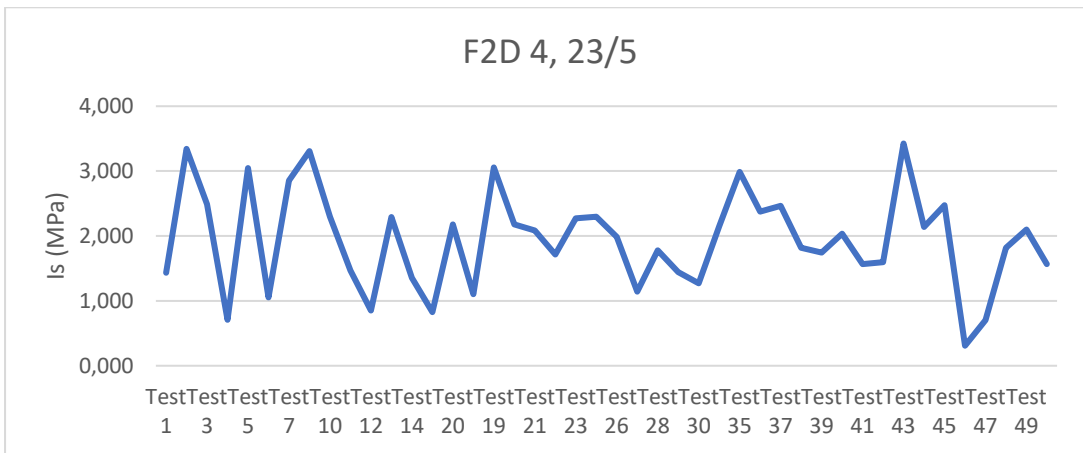


Figure 50 Point Load test for Blast 4 bench

11.4 ROCK MASS RATING

A. CLASSIFICATION PARAMETERS AND THEIR RATINGS

PARAMETER		Range of values // ratings							
1	Strength of intact rock material	Point-load strength index	> 10 MPa	4 - 10 MPa	2 - 4 MPa	1 - 2 MPa	For this low range uniaxial compr. strength is preferred		
		Uniaxial compressive strength	> 250 MPa	100 - 250 MPa	50 - 100 MPa	25 - 50 MPa	5 - 25 MPa	1 - 5 MPa	< 1 MPa
	RATING	15	12	7	4	2	1	0	
2	Drill core quality RQD	90 - 100%	75 - 90%	50 - 75%	25 - 50%	< 25%			
	RATING	20	17	13	8	5			
3	Spacing of discontinuities	> 2 m	0.6 - 2 m	200 - 600 mm	60 - 200 mm	< 60 mm			
	RATING	20	15	10	8	5			
4	Condition of discontinuities	Length, persistence	< 1 m	1 - 3 m	3 - 10 m	10 - 20 m	> 20 m		
		Rating	6	4	2	1	0		
		Separation	none	< 0.1 mm	0.1 - 1 mm	1 - 5 mm	> 5 mm		
		Rating	6	5	4	1	0		
		Roughness	very rough	rough	slightly rough	smooth	slickensided		
		Rating	6	5	3	1	0		
		Infilling (gouge)	none	Hard filling		Soft filling			
	-	< 5 mm	> 5 mm	< 5 mm	> 5 mm				
Rating	6	4	2	2	0				
Rating	6	5	3	1	0				
5	Ground water	Inflow per 10 m tunnel length	none	< 10 litres/min	10 - 25 litres/min	25 - 125 litres/min	> 125 litres /min		
		p_w / σ_1	0	0 - 0.1	0.1 - 0.2	0.2 - 0.5	> 0.5		
		General conditions	completely dry	damp	wet	dripping	flowing		
		RATING	15	10	7	4	0		

Figure 51 Rock Mass Rating, Classification of Rock Masses (Bieniaswki, 1989)

11.5 ROCK FACTOR

Table 13 Rock Factor Measurement Parameters (S.Gheibe, H.Aghababa, & S.H.Hoseini, 2009)

RMD		Rockmass Description
Powdery/Friable		10
Vertically Jointed		JF*
Massive		50
JPS		Vertical Joint Spacing
<0.1m		10
0.1m to MS		20
MS* to DP*		50
JPA		Joint Plane Angle
Dip out of face		20
Strike perpendicular to face		30
Dip into face		40
RDI		Rock Density Influence
RDI = 25 RD* -50		RD= rock density (t/m ³)
HF		Hardness Factor (GPa)
Y/3		if Y<50
UCS*/5		if Y>50
MEANING		Unit
MS	Oversize	m
DP	Drilling Pattern Size	m
Y	Young's Modulus	GPa
UCS	Uniaxial Compressive Strength	MPa
JF = JPS + JPA		

$$E_m = \sqrt{\frac{\sigma_c}{100}} 10^{\left(\frac{RMR-10}{40}\right)}$$

E_m = Modulus (GPa)

σ_c = UCS (MPa)

RMR = Rock Mass Rating

UCS = 24 x I_s (MPa)

I_s = Point Load Strength (MPa)

Rock Factor = 0,06 (RMD + RDI + HF) or 0,06 (JF + RDI + HF)

	ZONE 1/EX	ZONE 2/EX	Blast 1	Blast 2	Blast 3	Blast 3	Blast 4	
RMR	73,5	74,25	73,00	78,28	74,00	78,00	75,00	
GSI	68,50	69,25	68,00	73,28	69,00	73,00	70,00	
Y1	47,00	48,50	46,00	56,56	48,00	56,00	50,00	Gpa
Y2	38,68	40,39	37,58	50,93	39,81	50,12	42,17	Gpa
Y3	17,49	22,40	19,67	26,46	22,00	26,68	21,53	Gpa
UCS	36,34	54,72	48,72	48,00	54,31	50,40	46,37	Mpa
Is	1,51	2,28	2,03	2,00	2,26	2,10	1,93	Mpa
BURDEN	6,00	6,00	6,00	6,00	6,00	6,00	6,00	meter
SPACING	4,50	4,50	3,50	4,00	3,50	4,00	4,50	meter
HF1	15,67	16,17	15,33	18,85	16,00	18,67	16,67	
HF2	12,89	13,46	12,53	16,98	13,27	16,71	14,06	
HF3	5,83	7,47	6,56	8,82	7,33	8,89	7,18	
HF4 -UCS	7,27	10,94	9,74	9,60	10,86	10,08	9,27	
JF	50,00	45,00	45,00	50,00	45,00	50,00	50,00	
RDI	15,00	15,00	15,00	15,00	15,00	15,00	15,00	
A1	4,84	4,57	4,52	5,03	4,56	5,02	4,90	
A2	4,67	4,41	4,35	4,92	4,40	4,90	4,74	
A3	4,25	4,05	3,99	4,43	4,04	4,43	4,33	
A4	4,34	4,26	4,18	4,48	4,25	4,50	4,46	

Figure 52 Rock Factor Calculation; Green cells indicate the input data for measurement

	04-avr	15-mai	16-mai	15-avr	23-mai	16-juin
JF	45	50	45	50	50	50
P	4,58258	4,89898	4,58258	4,89898	5,19615	5,19615
JPS	20	20	20	20	20	20
JCF	1	1	1	1	1	1
JPA	25	30	25	30	30	30

Figure 53 Supporting Data for Rock Factor Calculation

11.6 EXPLOSIVES

Table 14 Explosives characteristics

Characteristics	Senatel	Eurodyn	ANFO
Diameter	85 mm	85 mm	-
Mass	3,125 kg	5 kg	-
Length	470 mm	620 mm	-
Velocity on Detonation	6050 m/s ²	6200 m/s ²	3800 m/s ² (approx.)
Avg Density	1,2 kg/m ³	1,4 kg/m ³	0,85 kg/m ³
Relative Weight Strength	134	145	100
Relative Bulk Strength	201	254	100

11.7 REGRESSION ANALYSIS



Figure 54 Regression Analysis for Blast 1, 4/4/19

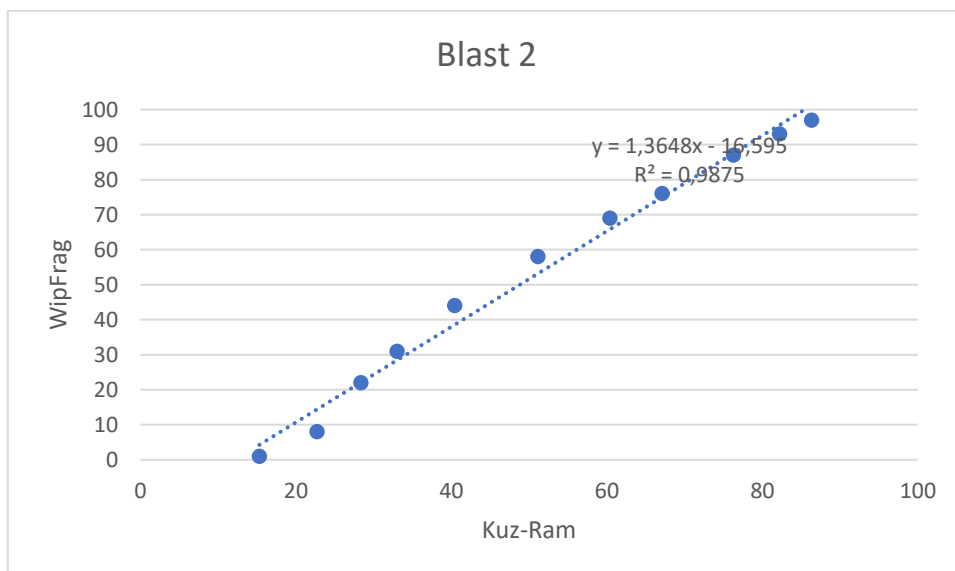


Figure 55 Regression Analysis for Blast 2, 15/5/19

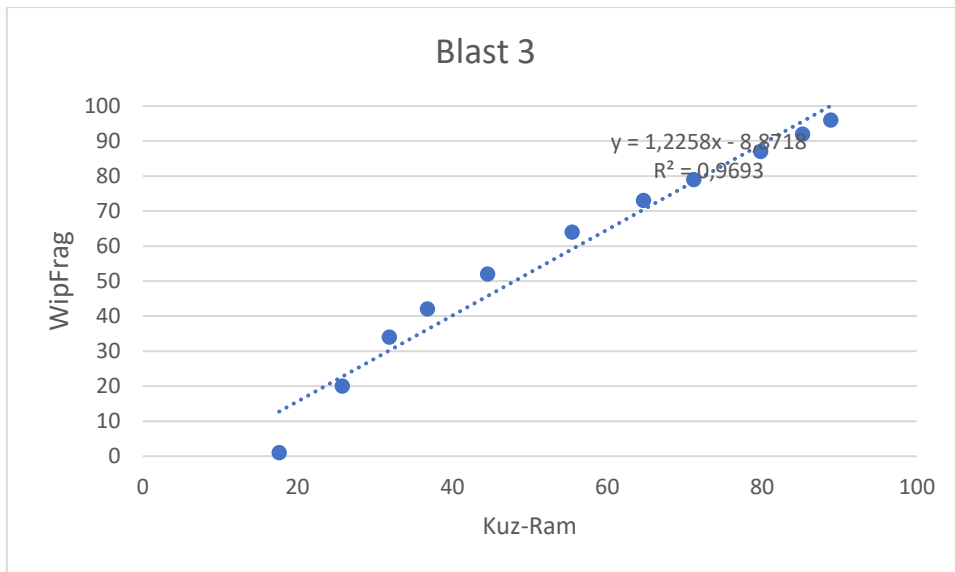


Figure 56 Regression Analysis for Blast 3, 16/5/19

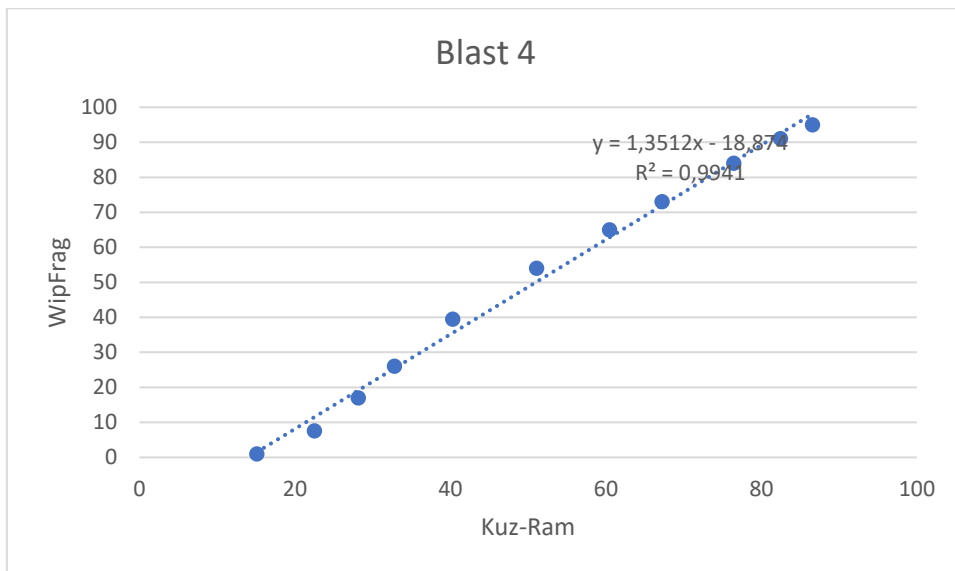


Figure 57 Regression Analysis for Blast 4, 23/5/19

11.8 FINES AREA CALCULATION

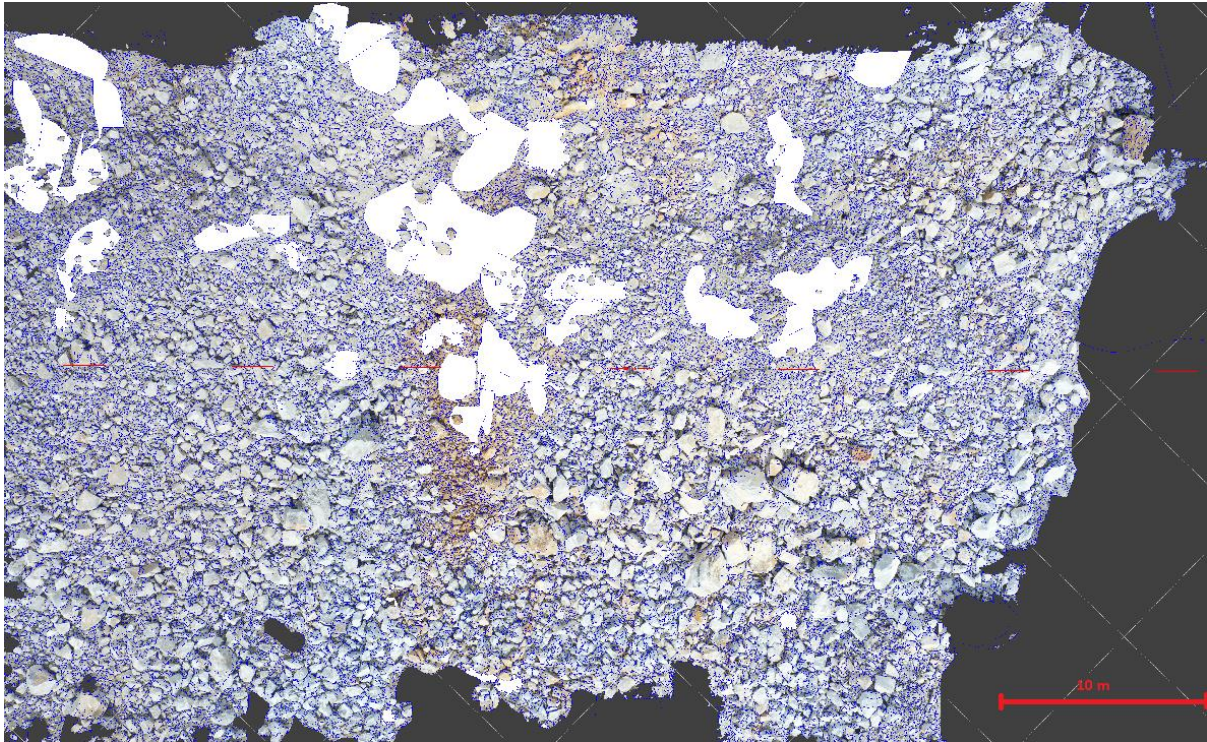


Figure 58 Image of Fragmentation, with white region distinguishing the fines area.

The total area of the fragmentation is calculated using inscribed circles, for example, in the figure above the dimensions are 58 m x 36 m . So we inscribe circles with in it; one of diameter 36 m then add another with 22 m dia circle and furthermore the remaining space is filled with circles of dia 14m and two of 7 m.

The area calculated from region of fines is divided with the total area measured from the inscribed circle method is referred to as the percentage of fines for the region.

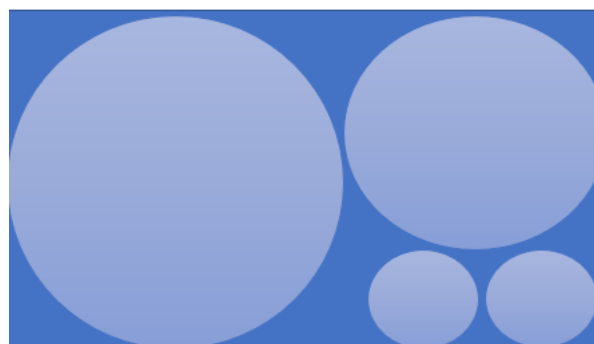


Figure 59 Schematic of inscribed circle method

11.9 ROCK MASS TRACING

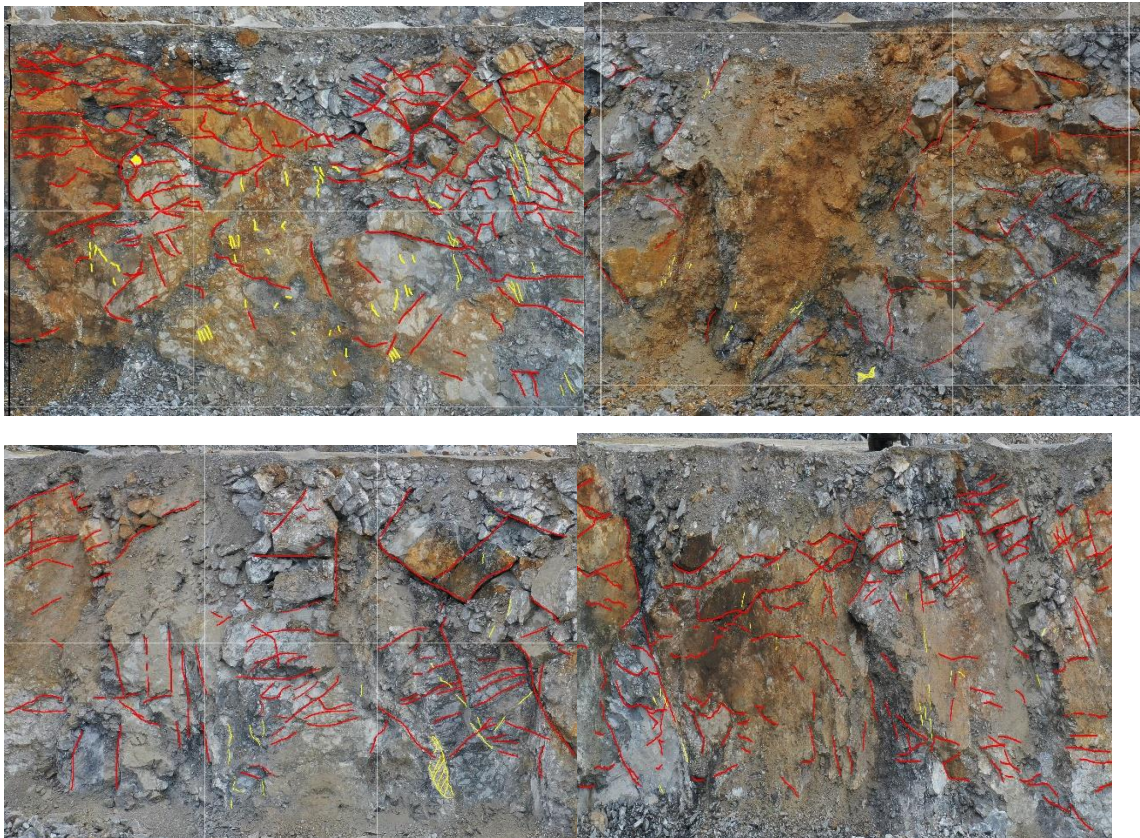


Figure 60 Rock Mass Discontinuity Tracing using ImageJ; 4/4/19, For scale use Grid Size, 5m x 5m

Table 15 Average RMR values for each zone in Bench Blasted 4/4/19

Zone	RMR
Z 1	68,43
Z 2	75,17
Z 3	71,80
Z 4	73,40
Average	72,00

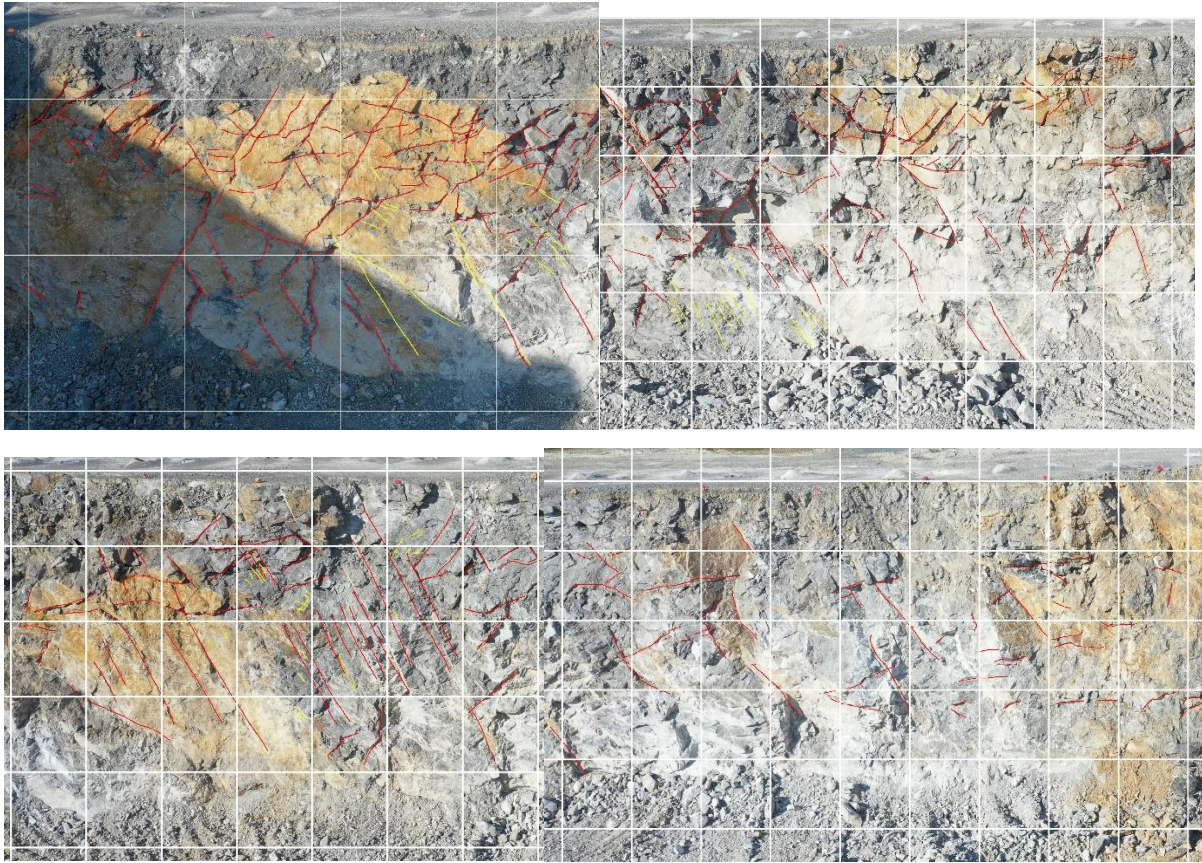


Figure 61 Rock Mass Discontinuity Tracing using ImageJ; 15/5/19, for scale use Grid size 2m x 2m

Table 16 Average RMR values for each zone in Bench Blasted 15/5/19

Zone	RMR
Z 1	79,25
Z 2	76,50
Z 3	78,25
Z 4	76,75
Average	77,68

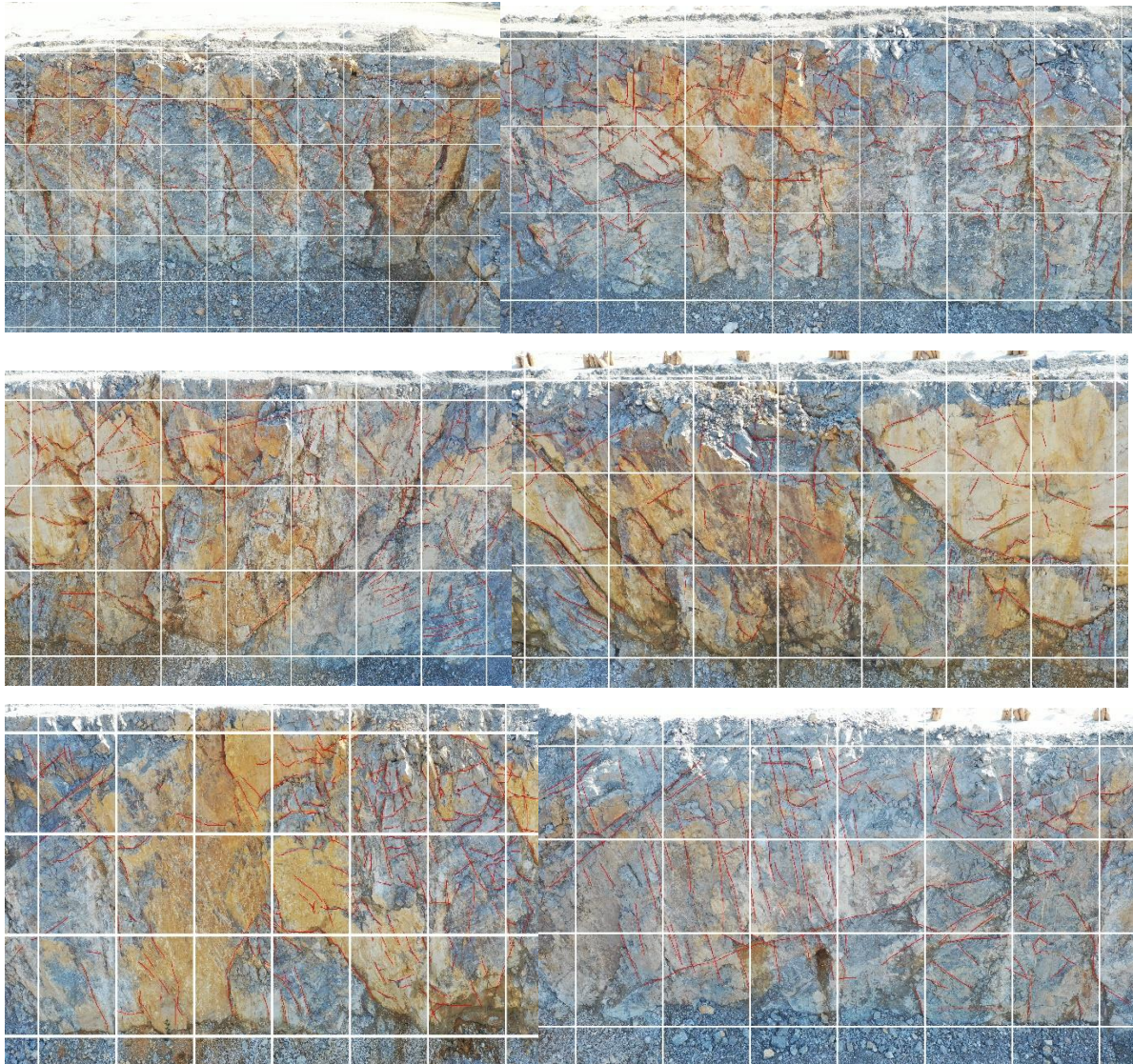


Figure 62 Rock Mass Discontinuity Tracing using ImageJ; 23/5/19; For scale use Grid Size 4m x 4m

Table 17 Average RMR values for each zone in Bench Blasted 23/5/19

Zone	RMR
Z-1	74,25
Z-2	71,75
Z-3	76,75
Z-4	76,25
Z-5	79,75
Z-6	73,50
Z-7	73,75
Average	75,14

11.10 FRAGMENTATION



Figure 63 Fragmentation from Blast 1

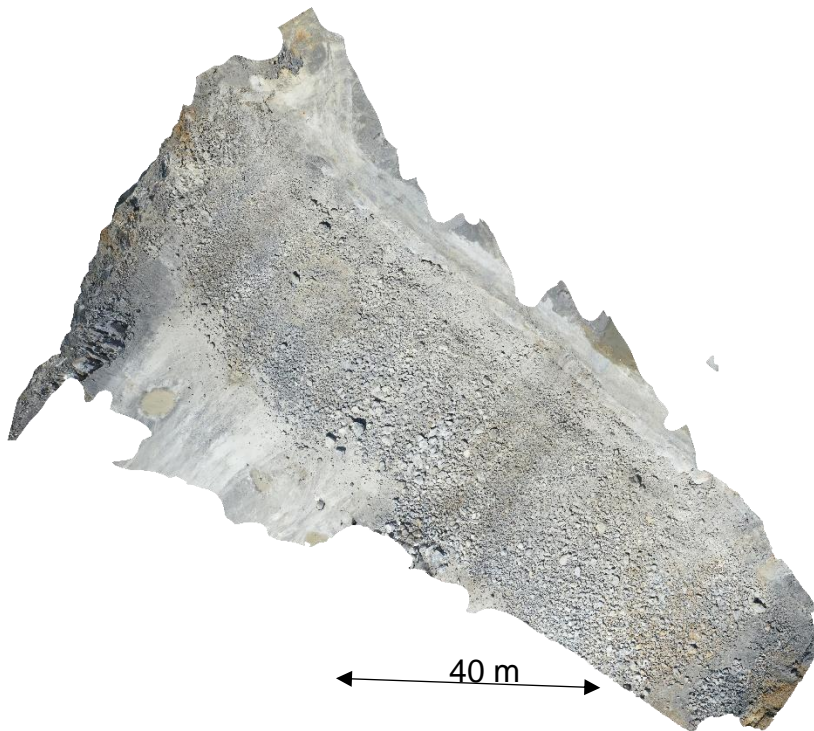


Figure 64 Fragmentation from Blast 2



Figure 65 Fragmentation From Blast 3



Figure 66 Fragmentation from Blast 4